Search for Neutrinoless Double Beta Decay in Liquid Xenon TPCs

Zepeng Li, Yale University

Neutrino mass generation

- Neutrino oscillations require that neutrinos have non-zero mass.
- Neutrino mass is significantly smaller than the other fermions.
- If neutrinos are Majorana particles, see-saw mechanism provides a natural explanation of small neutrino mass.

The Standard Model fermion masses

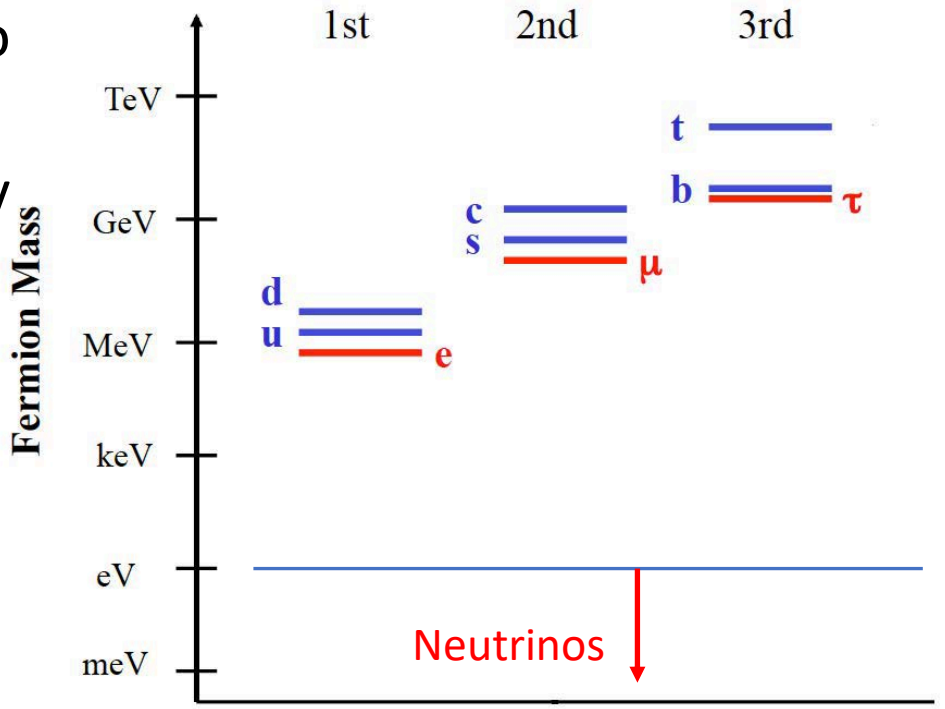

Double beta decay

Observable if single beta decay is forbidden

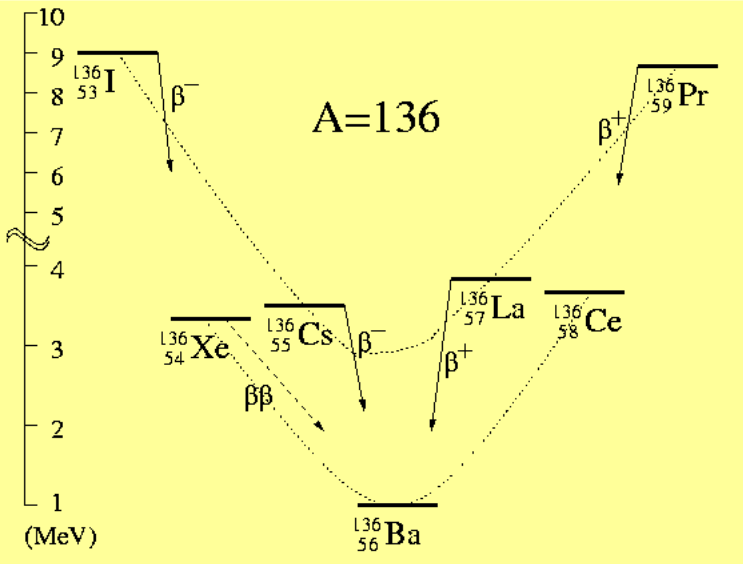

Examples with Q>2MeV

Candidate	Q (MeV)	Abundance
^{48}Ca→^{48}Ti	4.271	0.187
^{76}Ge→^{76}Se	2.040	7.8
^{82}Se→^{82}Kr	2.995	9.2
^{96}Zr→^{96}Mo	3.350	2.8
^{100}Mo→^{100}Ru	3.034	9.6
^{110}Pd→^{110}Cd	2.013	11.8
^{116}Cd→^{116}Sn	2.802	7.5
^{124}Sn→^{124}Te	2.228	5.64
^{130}Te→^{130}Xe	2.533	34.5
^{136}Xe→^{136}Ba	2.458	8.9
^{150}Nd→^{150}Sm	3.367	5.6

$$T_{1/2}^{2\nu} \sim 2 \times 10^{21} y$$

Neutrinoless Double Beta Decay

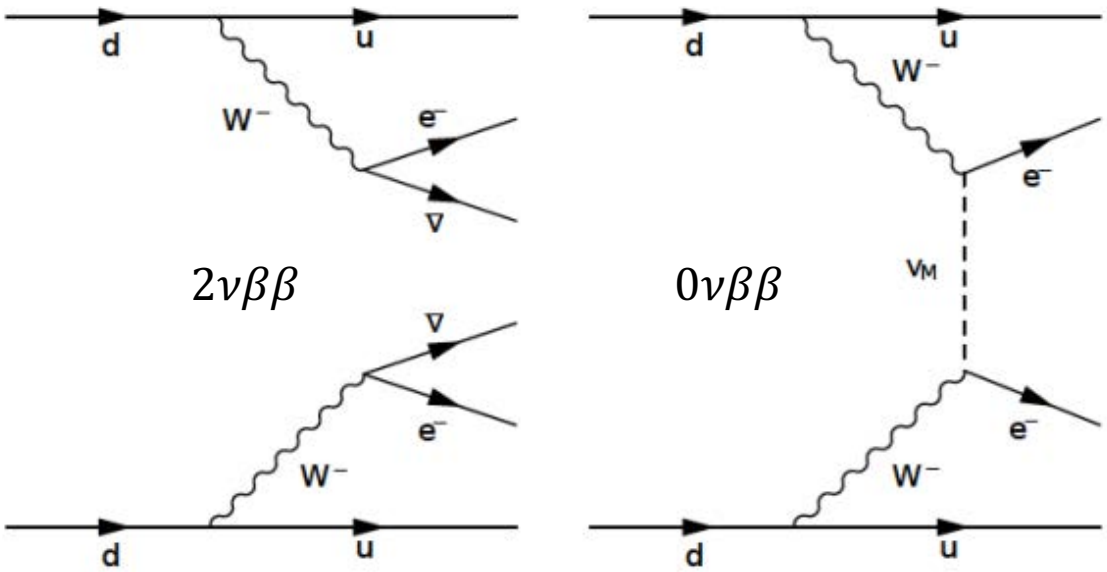

The **neutrinoless mode** ($0\nu\beta\beta$) can only happen if neutrinos are Majorana particles.

The observation of this hypothetical decay would prove violation of lepton number and constrain the absolute neutrino mass scale.

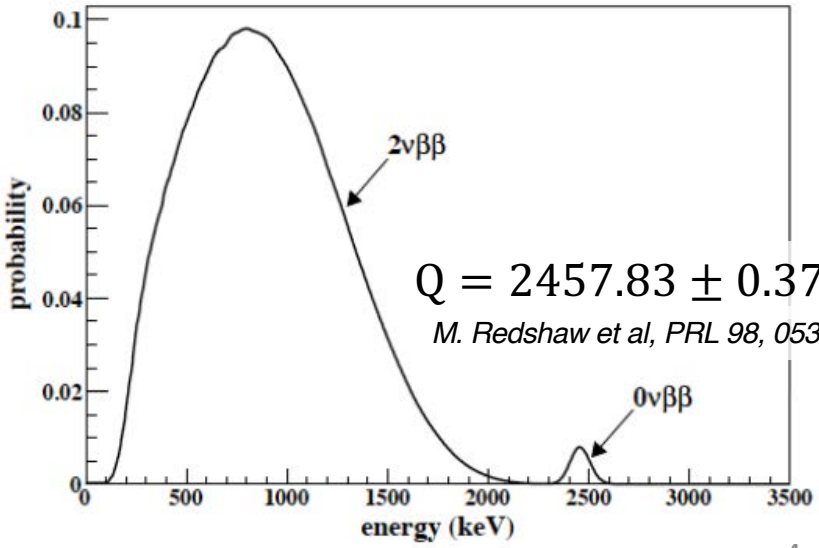

$Q = 2457.83 \pm 0.37$ keV

M. Redshaw et al, PRL 98, 053003 (2007)

Neutrinoless double beta decay experiments

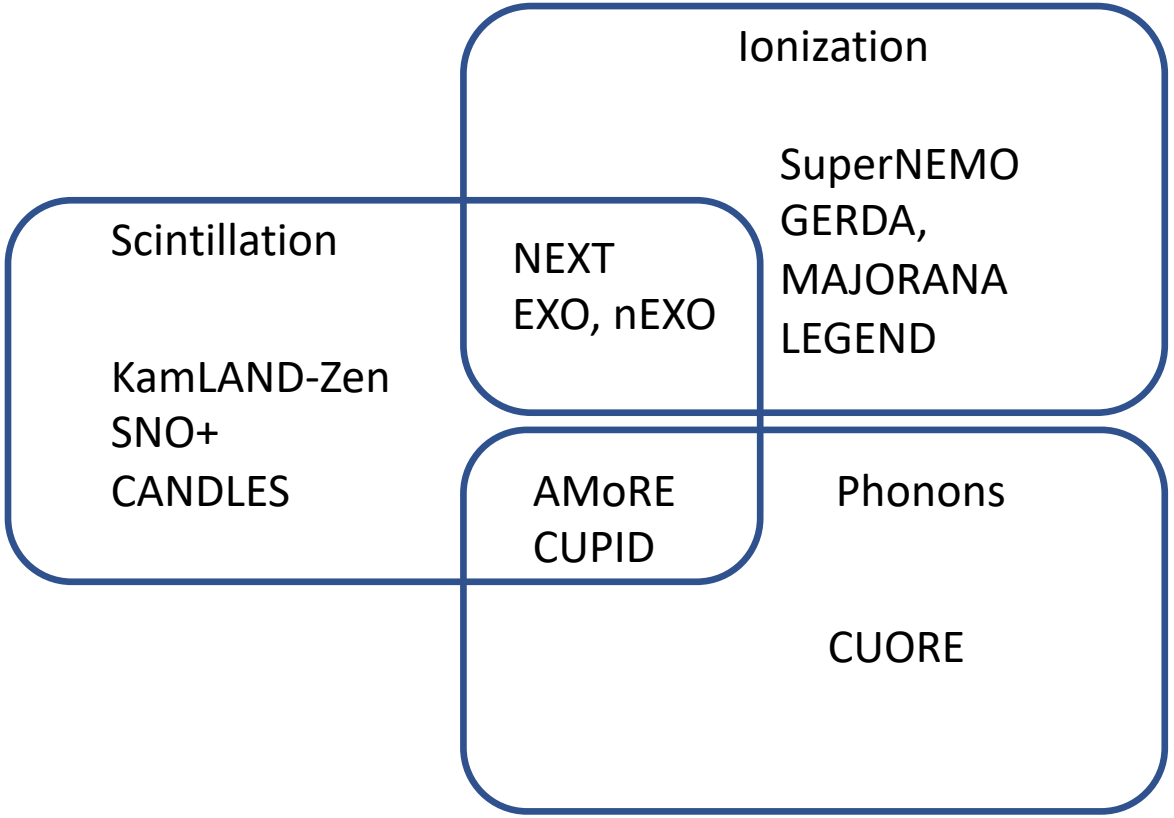

This is not an exhaustive list of neutrinoless double beta decay experiments.

The EXO-200 detector

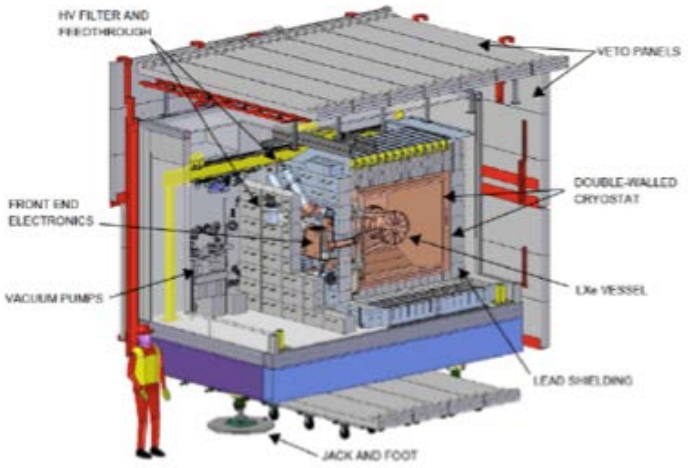

Located at the Waste Isolation Pilot Plant, Carlsbad NM

- **1585 m.w.e. overburden**
- Low levels of U/Th (compared to rock) and Rn

~150 kg of liquid Xenon enriched to 80.6% in ^{136}Xe

- High Q-value above most γ backgrounds
- Provides self shielding

Time projection chamber inside Cu cryostat

- Split in two equal halves with common cathode
- **U- and V-wires for charge readout, APDs for light collection**
- All materials have been screen for radio-purity

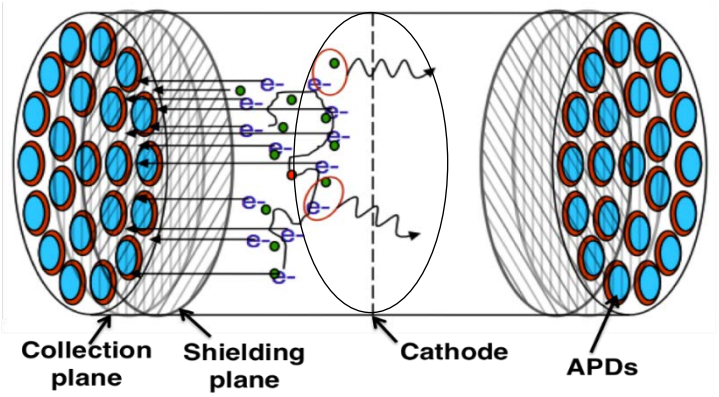

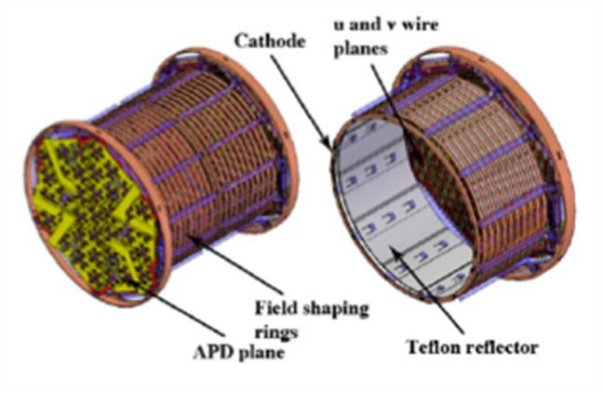

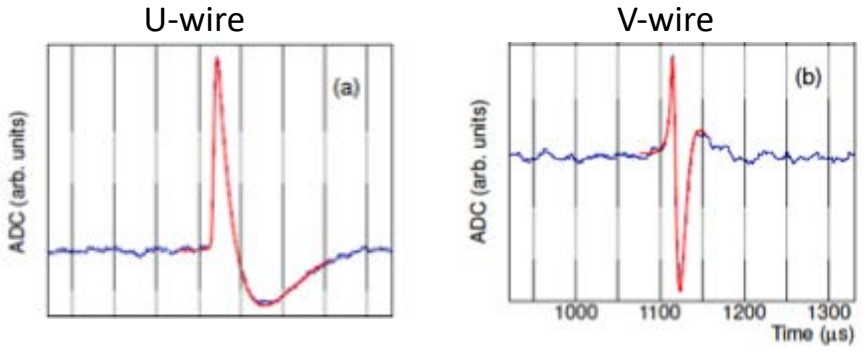

Energy Reconstruction

- Using anti-correlation between charge and scintillation response
  Rotated energy provides optimal resolution in the energy of interest

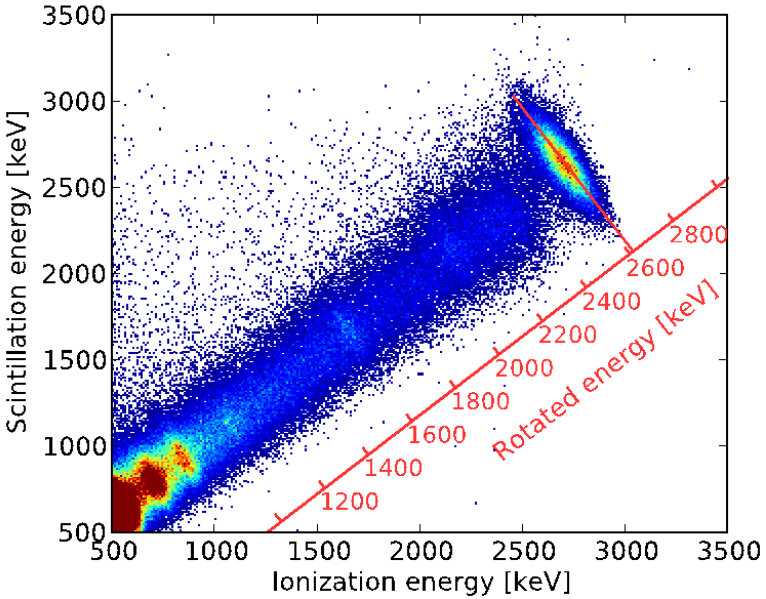

Spatial-time average resolutions:

Phase I: $1.35 \pm 0.09\%$
Phase II: $1.15 \pm 0.02\%$

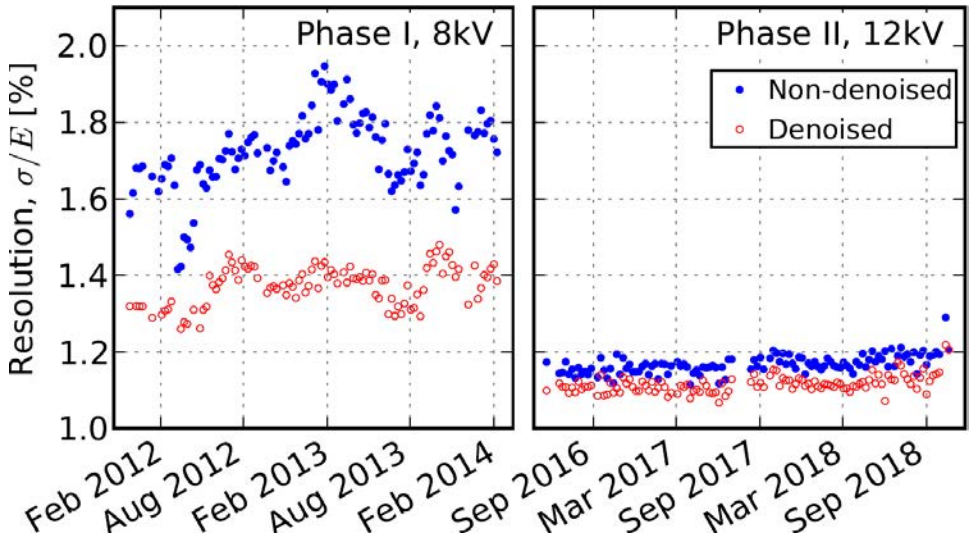

New front end readout electronics
Reduce APD readout excess noise
Proper modeling of mixed collection/induction wire signals

Position Discrimination

- $\beta\beta$ deposits energy at single location
- TPC allows the rejection of gamma backgrounds because Compton scattering results in multiple energy deposits.

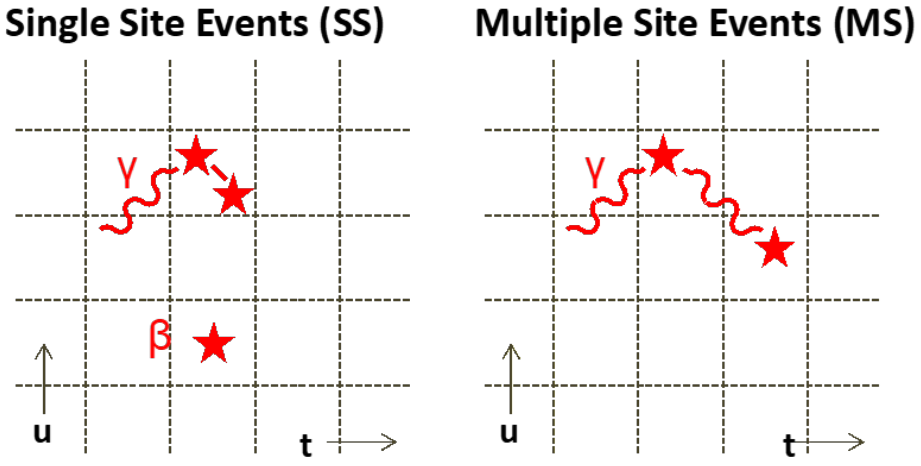

SS fraction ~ 12% in the energy region of interest

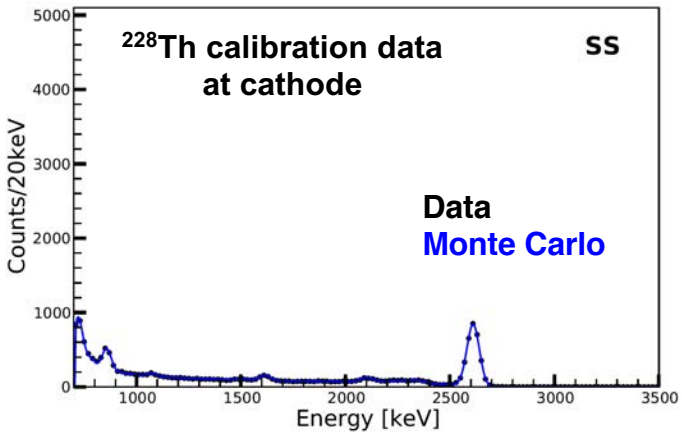

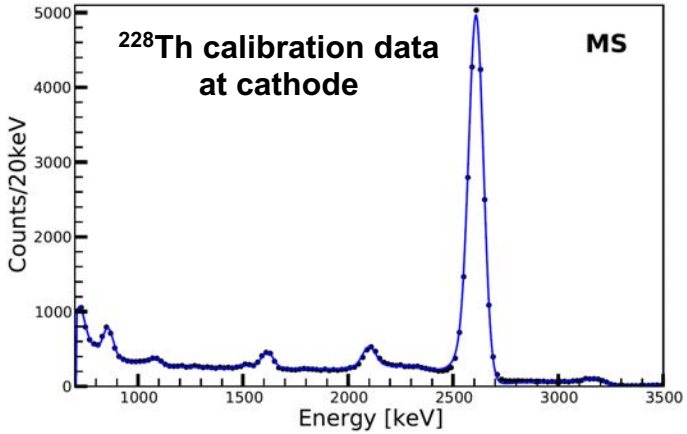

EXO-200 Best-fit Result

arXiv: 1906.02723

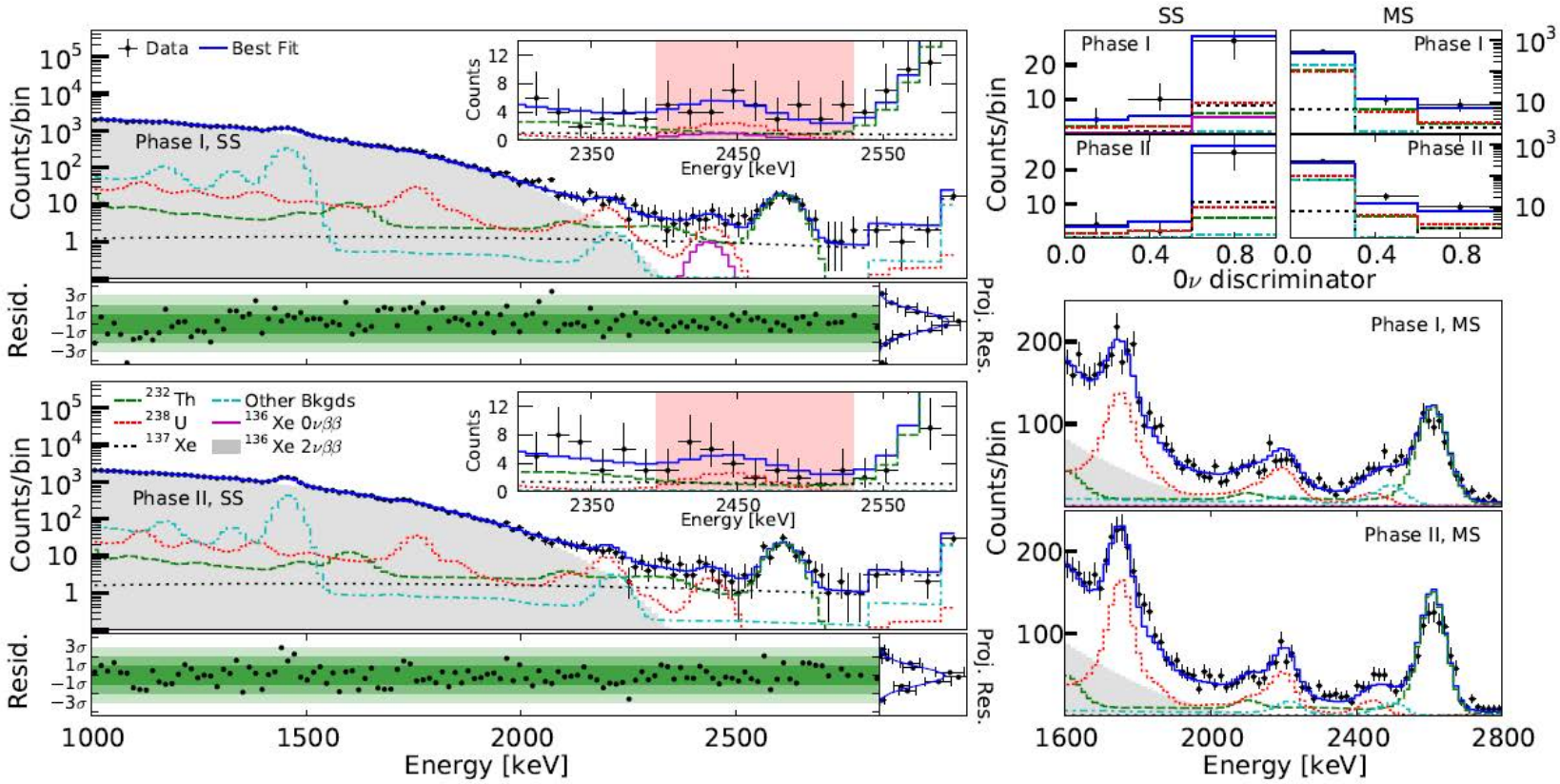

Background contribution to Q $\pm$ 2σ

(counts)	^{238}U	^{232}Th	^{137}Xe	Total	Data
Phase I	12.6	10.0	8.7	32.3±2.3	39
Phase II	12.0	8.2	9.3	30.9±2.4	26

EXO-200 Full Dataset Results

Phase I+II: 234.1 kg·yr ^{136}Xe exposure

Limit $T_{1/2}^{0\nu\beta\beta} > 3.5 \times 10^{25}$ yr (90% C.L.)

$\langle m_{\beta\beta} \rangle < (93 - 286)$ meV

Sensitivity 5.0×10^{25} yr

No statistical significant signal observed

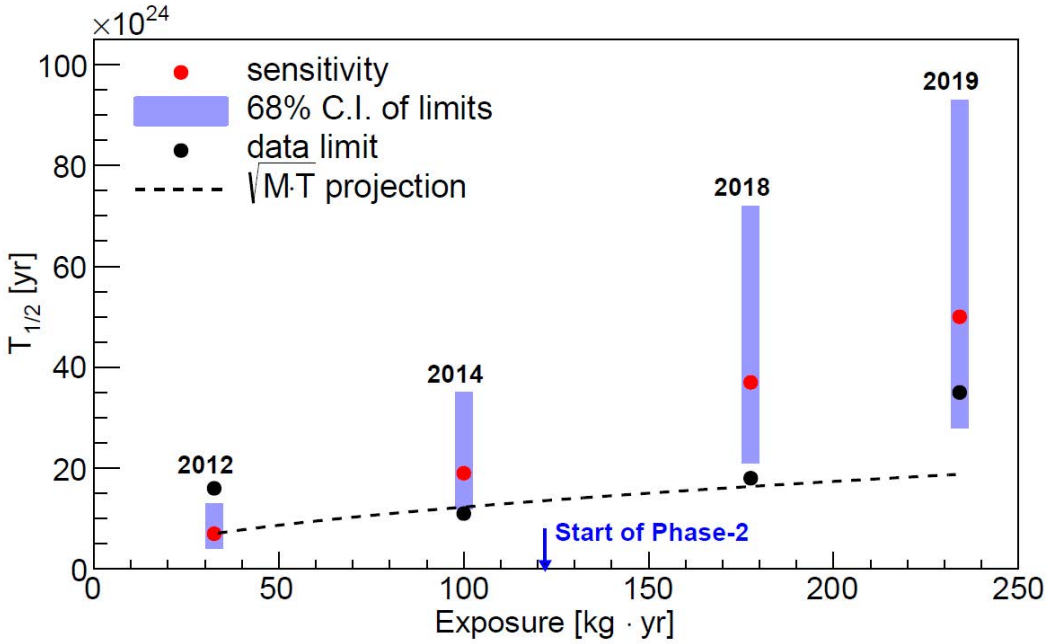

2012: Phys.Rev.Lett. 109 (2012) 032505
2014: Nature 510 (2014) 229-234
2018: Phys. Rev. Lett. 120, 072701 (2018)
2019: arXiv 1906.02723

nEXO experiment

- nEXO is a proposed experiment to search for 0νββ decay of ^{136}Xe. Design based on the success of EXO-200.
- It will utilize ~5 tons of enriched LXe in a TPC.
- A large monolithic TPC will be used in nEXO. The chamber has a dimension of 1.25 m H x 1.16 m ⌀.

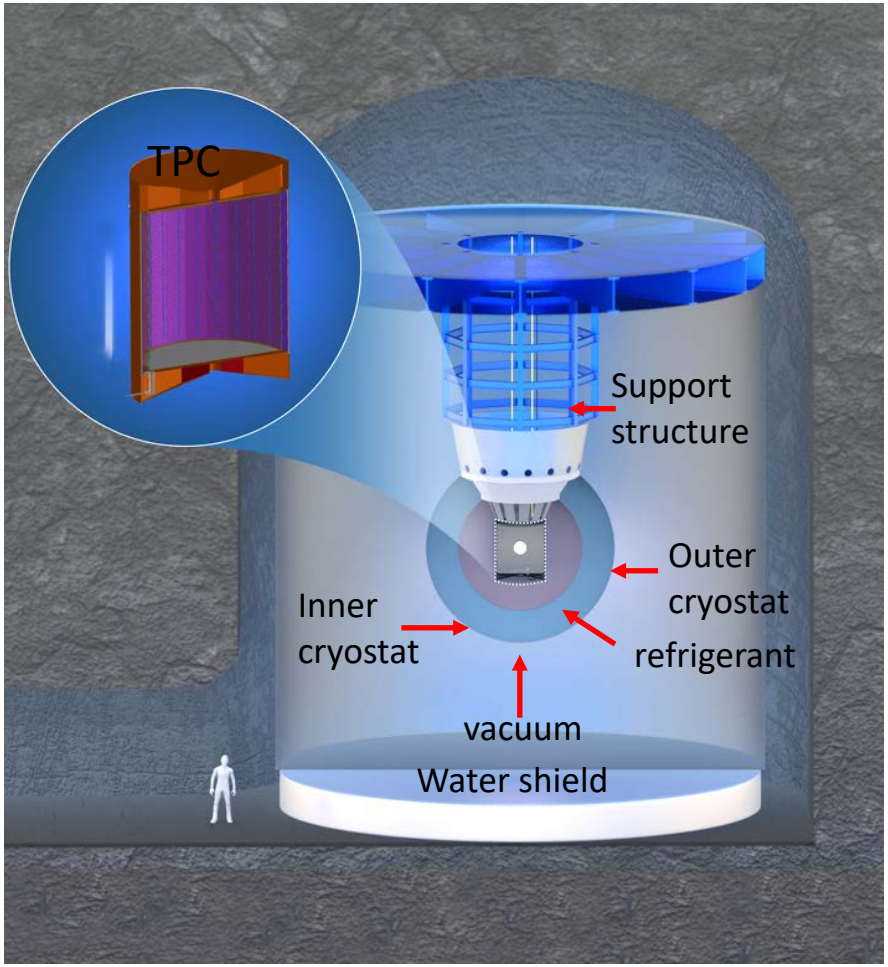

Segmented charge readout with tiles in nEXO

- A charge tile is designed for charge readout in nEXO. The tile does not need Frisch grid or wire tensioning support structure.
- The anode is composed of modularized tiles that reduces the ambiguity of hits.
- Built-on electronics on back using cold electronics technique.
- Test of prototype charge tile shows good performance.

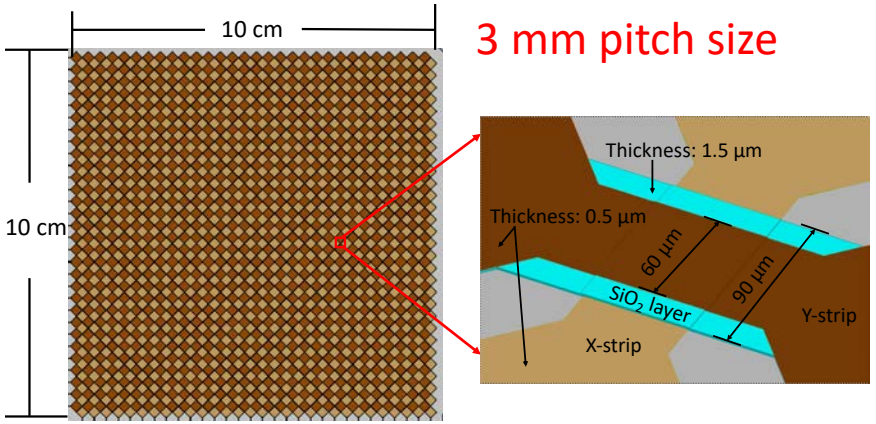

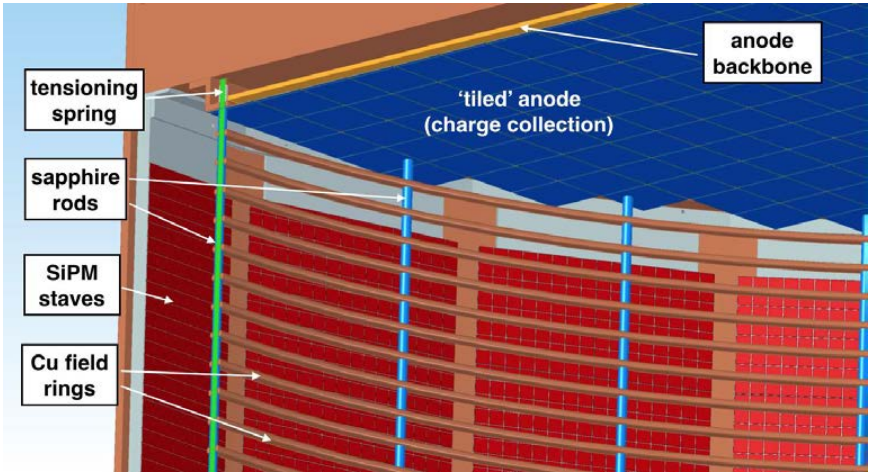

Schematic drawing of tiles mounting

VUV SiPM arrays for photon detection

- ~4.5 m^2 of VUV SiPMs on the barrel for photon detection.
- ASIC electronics in LXe.
- Simultaneous readout of ionization and scintillation.

Prototype VUV SiPM array

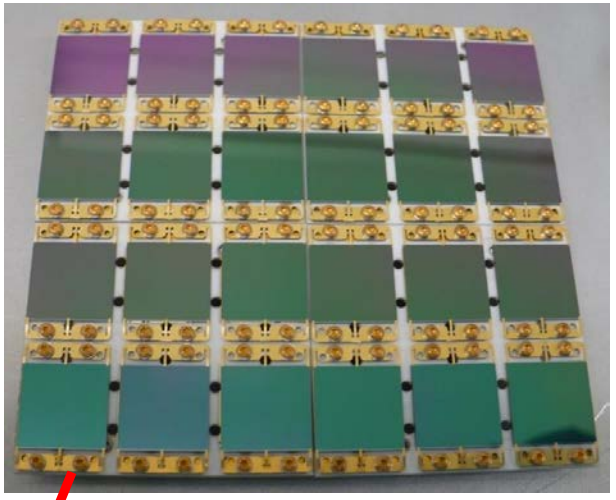

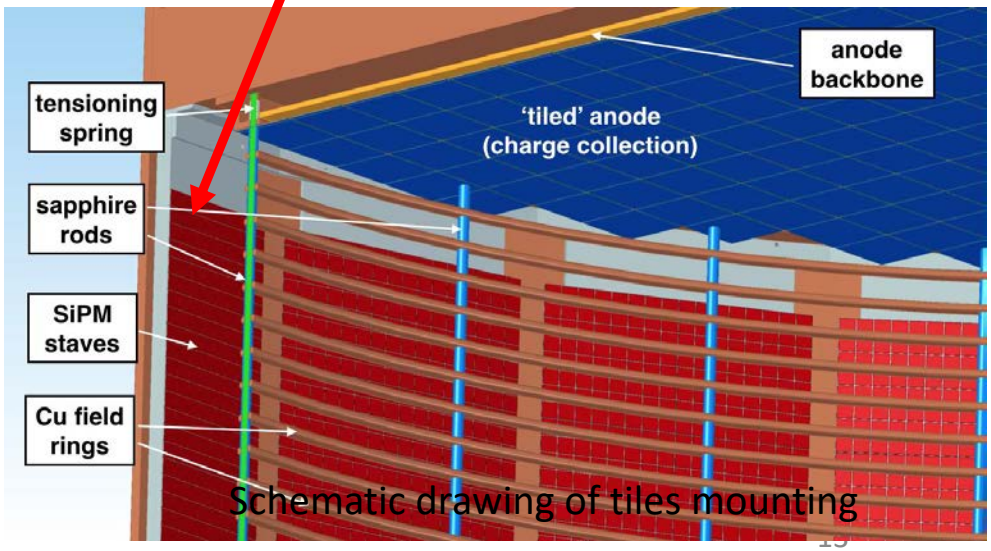

Schematic drawing of tiles mounting

nEXO compared to EXO-200

Optimization	Why
~30x volume/mass	To give sensitivity to the inverted hierarchy
No cathode in the middle	Larger low background volume/no ^{214}Bi in the middle
6x HV for the same field	Larger detector and one drift cell
>3x electron lifetime	Larger detector and one drift cell
Better photodetector coverage	Energy resolution
SiPM instead of APDs	Higher gain, lower bias, lower mass, E resolution
In LXe electronics	Lower noise, more stable, fewer cables/feedthroughs, E resolution, lower threshold for Compton ID
Lower outgassing materials	Longer electron lifetime
Different calibration methods	Very “deep” detector (by design)
Deeper site	Less cosmogenic activation
Larger vessels	5 ton detector and more shielding

nEXO sensitivity

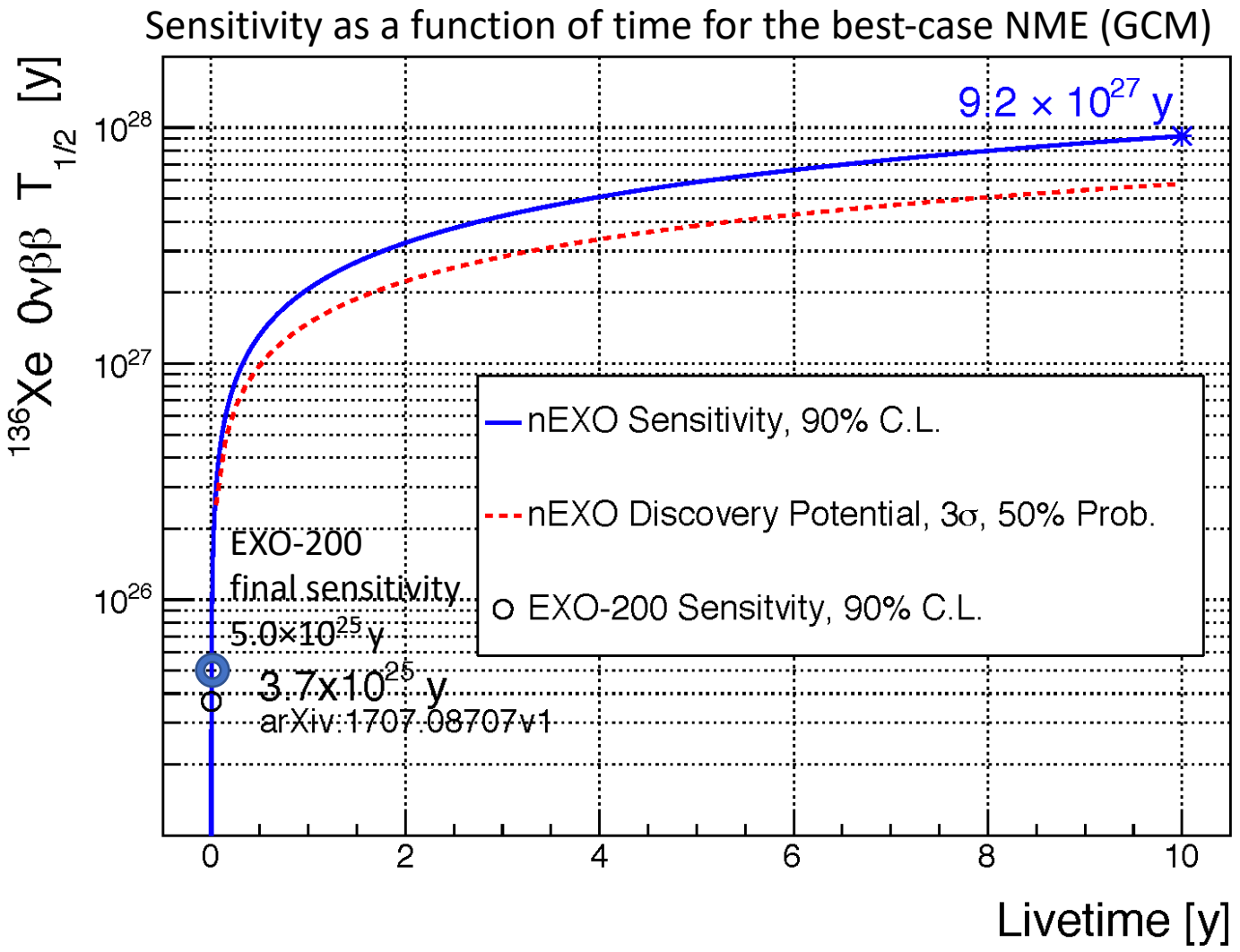

Barium tagging to confirm a double beta decay

- R&D work has demonstrated the feasibility of barium tagging.
- Ba tagging could become a long term nEXO upgrade, significantly extending sensitivity.

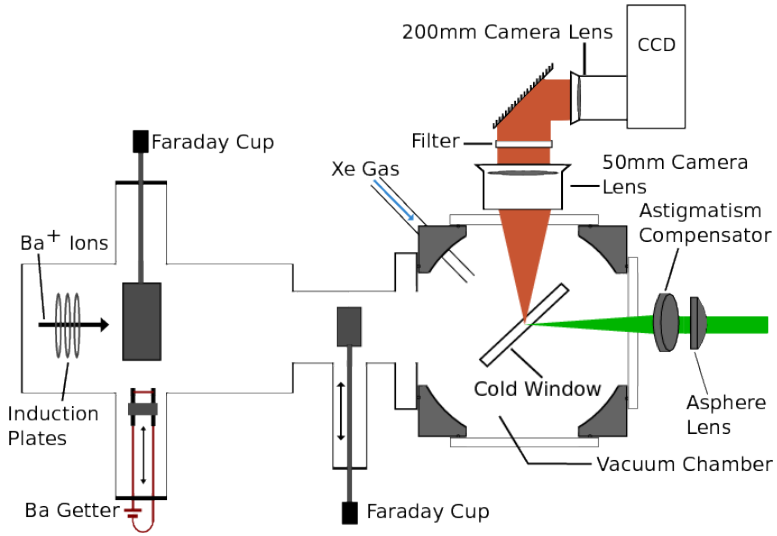

Accelerator deposits a few atoms in the SXe matrix

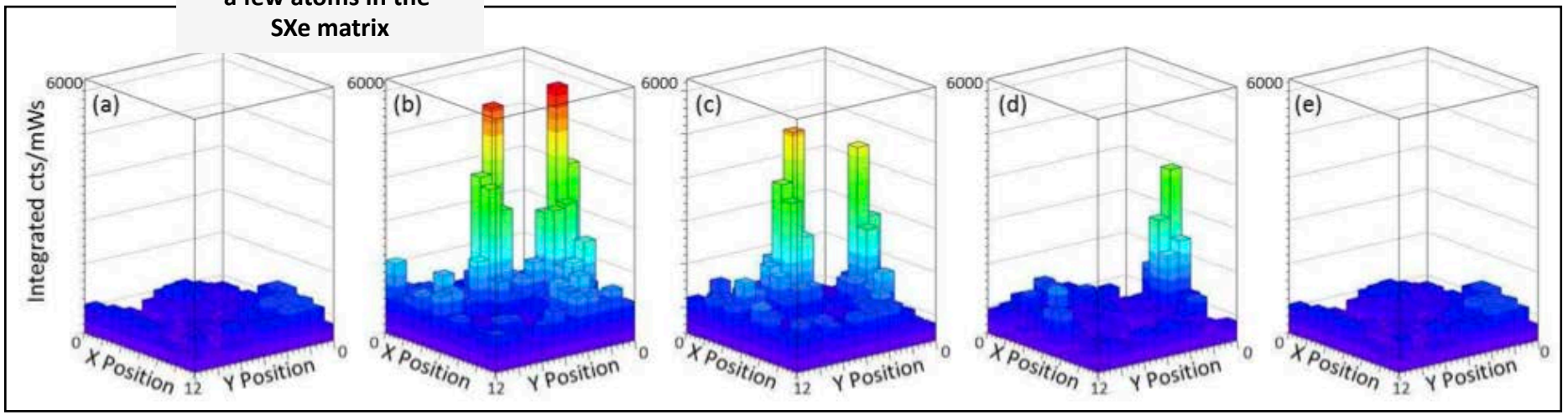

C.Chambers et al. Nature 569 (2019) 203

nEXO compared to EXO-200

Optimization	Why
~30x volume/mass	To give sensitivity to the inverted hierarchy
No cathode in the middle	Larger low background volume/no ^{214}Bi in the middle
6x HV for the same field	Larger detector and one drift cell
>3x electron lifetime	Larger detector and one drift cell
Better photodetector coverage	Energy resolution
SiPM instead of APDs	Higher gain, lower bias, lower mass, E resolution
In LXe electronics	Lower noise, more stable, fewer cables/feedthroughs, E resolution, lower threshold for Compton ID
Lower outgassing materials	Longer electron lifetime
Different calibration methods	Very “deep” detector (by design)
Deeper site	Less cosmogenic activation
Larger vessels	5 ton detector and more shielding

Charge signal readout in LXe TPC

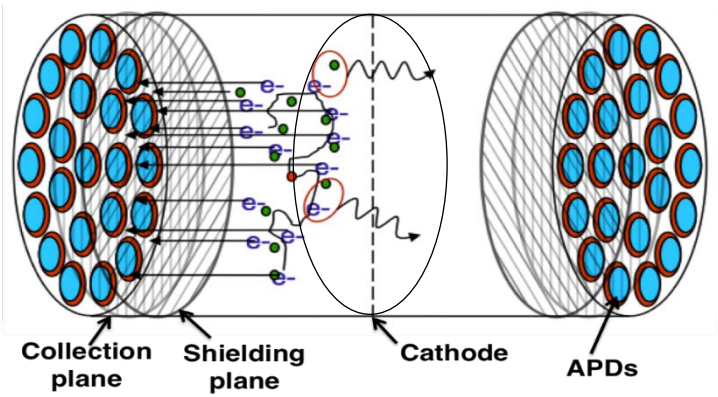

Electron lifetime in EXO-200 Phase-II

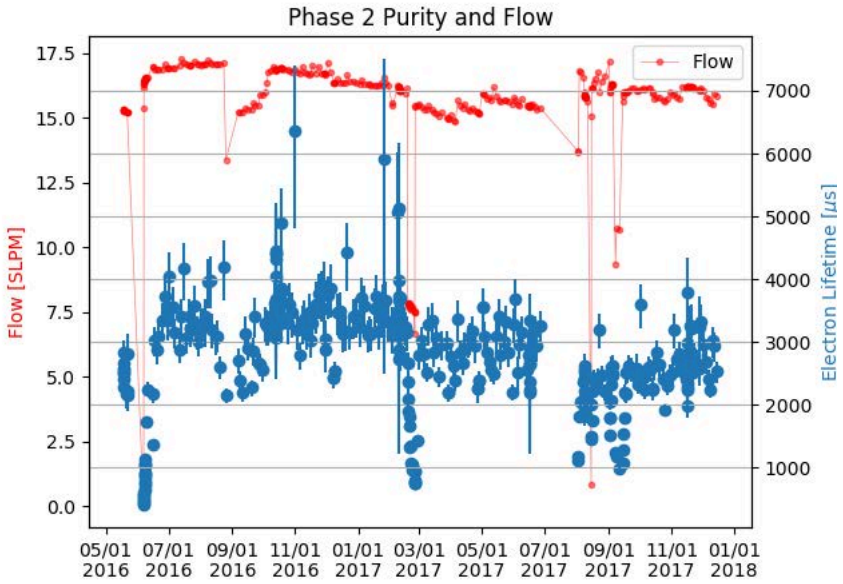

- Ionization electrons drift towards anode in the electric field.
- Electrons could be attached to electronegative impurities.

Ultrapure liquid xenon to achieve long electron lifetime

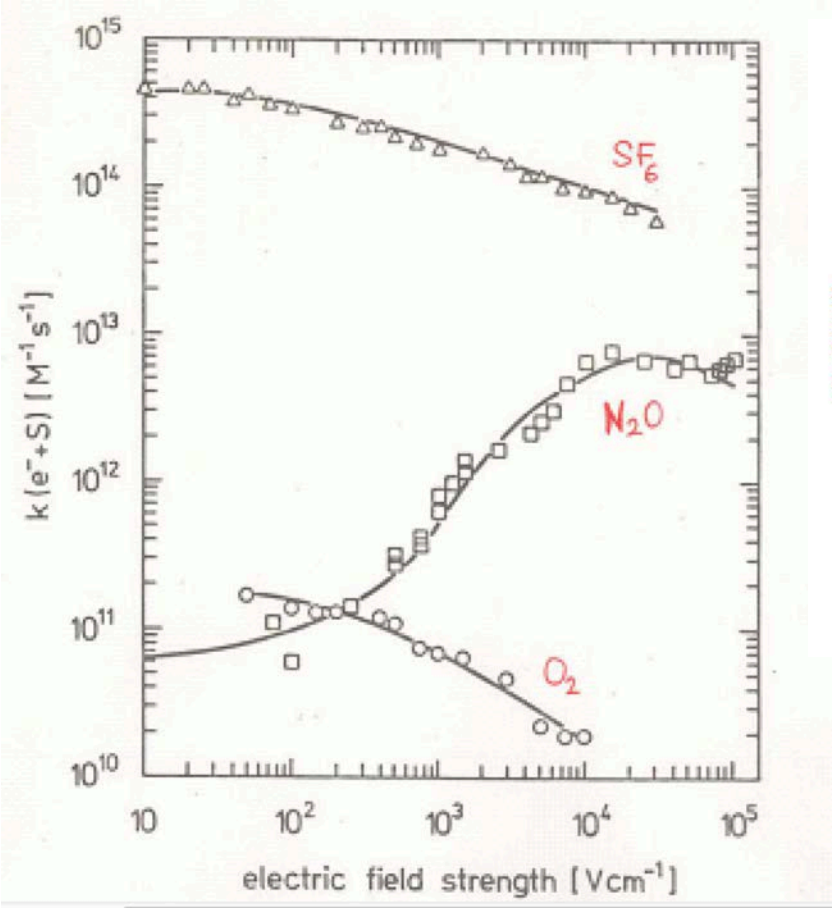

Electron lifetime in EXO-200 Phase-II

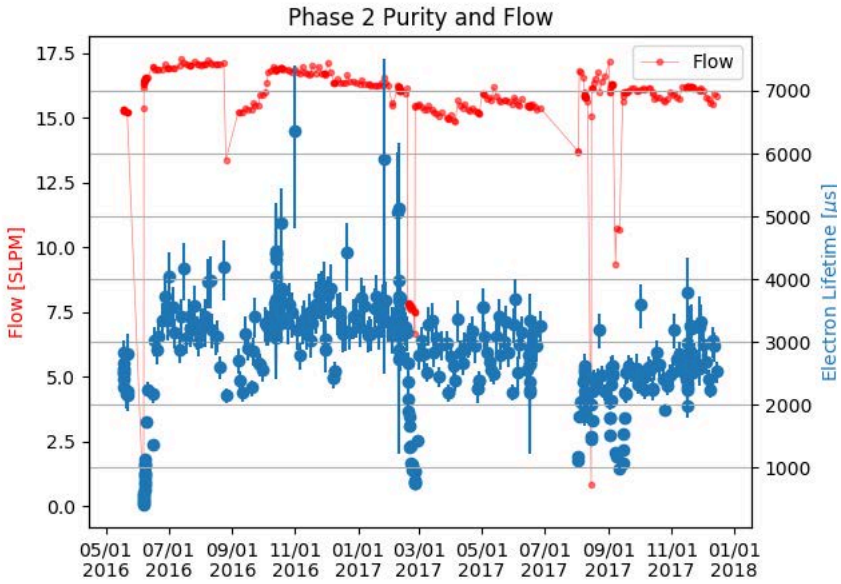

nEXO plans to achieve 10 ms electron lifetime!

J.Phys. Chem. 80 (1976) 2556

Lab measurement of electron lifetime and impurities

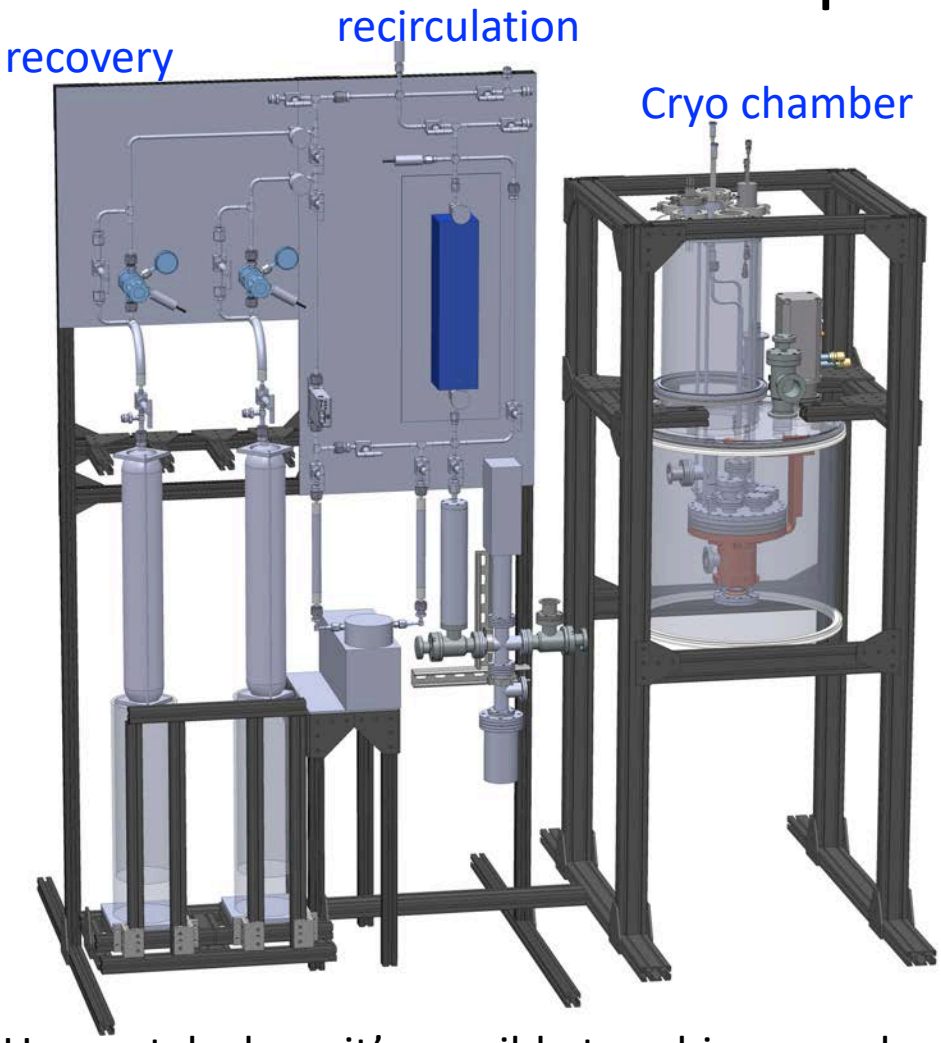

Use metal where it's possible to achieve good purity

Lab mesurement of electron lifetime and impurities

15 cm drift length
Plan to install a 30 cm long TPC

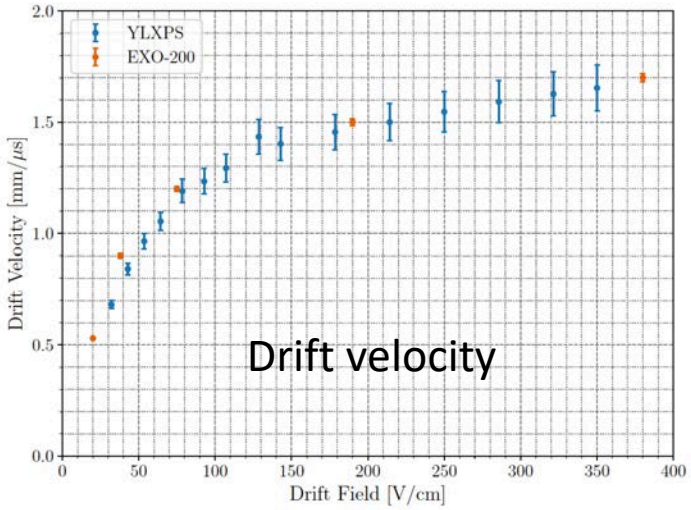

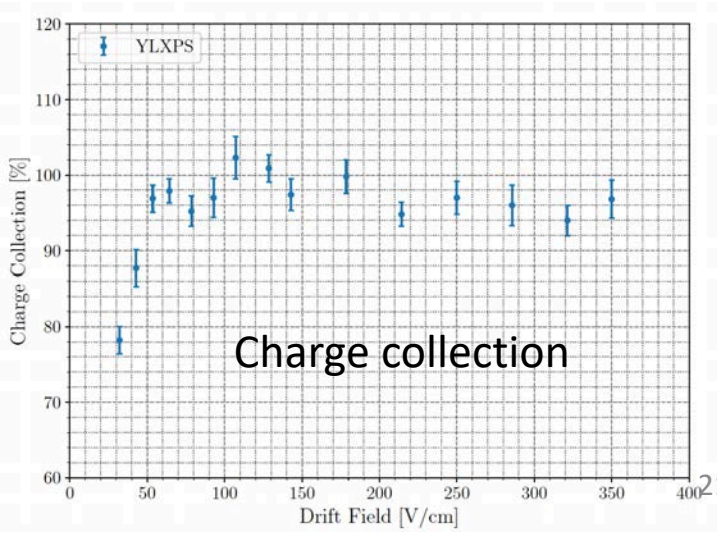

Lab measurement of material outgassing

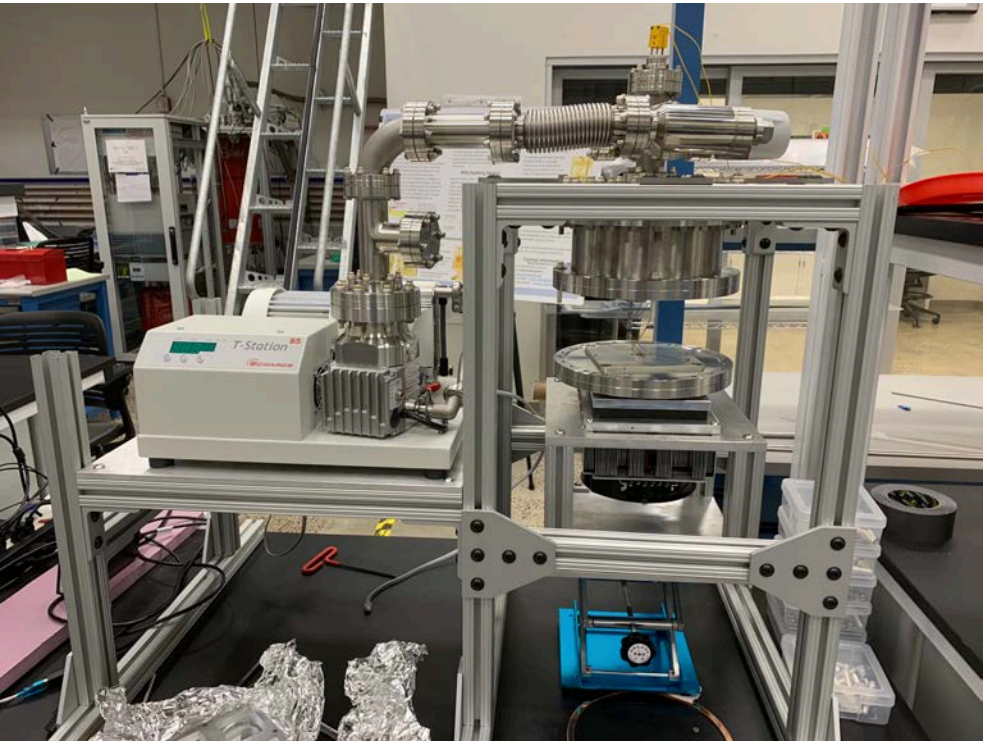

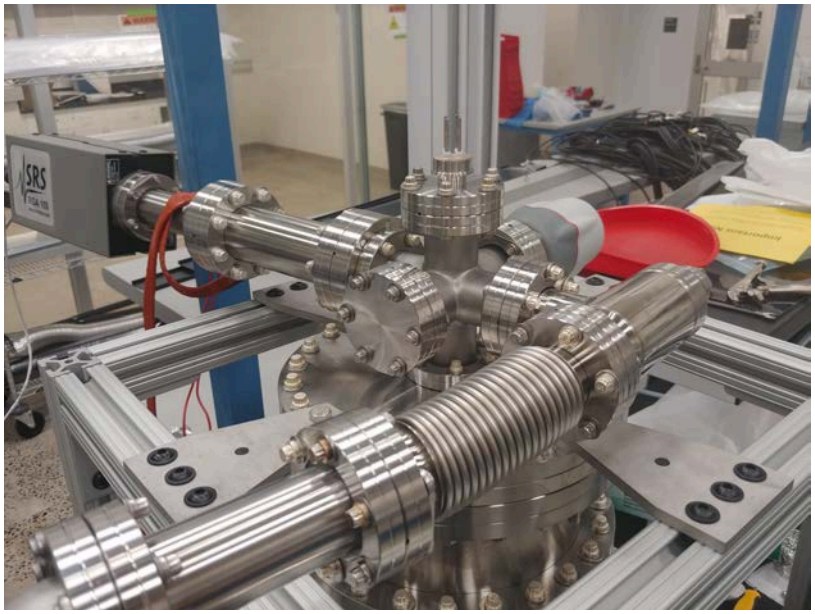

- Throughput method to measure the rate
- Conductance of pumping pipe calibrated
- Use RGA measure partial pressures

Lab measurement of material outgassing

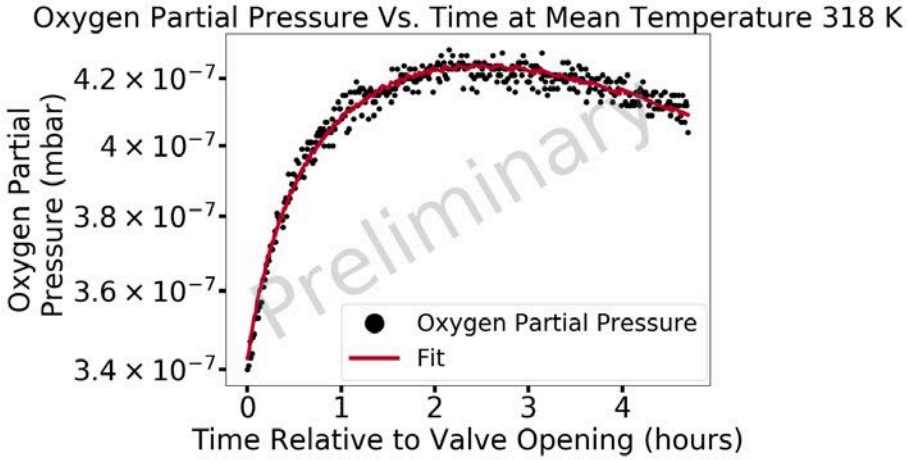

$$p(t,T) = A \cdot \exp(-\frac{b}{T}) \cdot \exp(-c \cdot t \cdot \exp(-\frac{b}{T}))$$

We can measure the activation energy of material that characterize its outgassing rate in the lab, and screen the materials to be used in nEXO.

Charge signal readout in LXe TPC

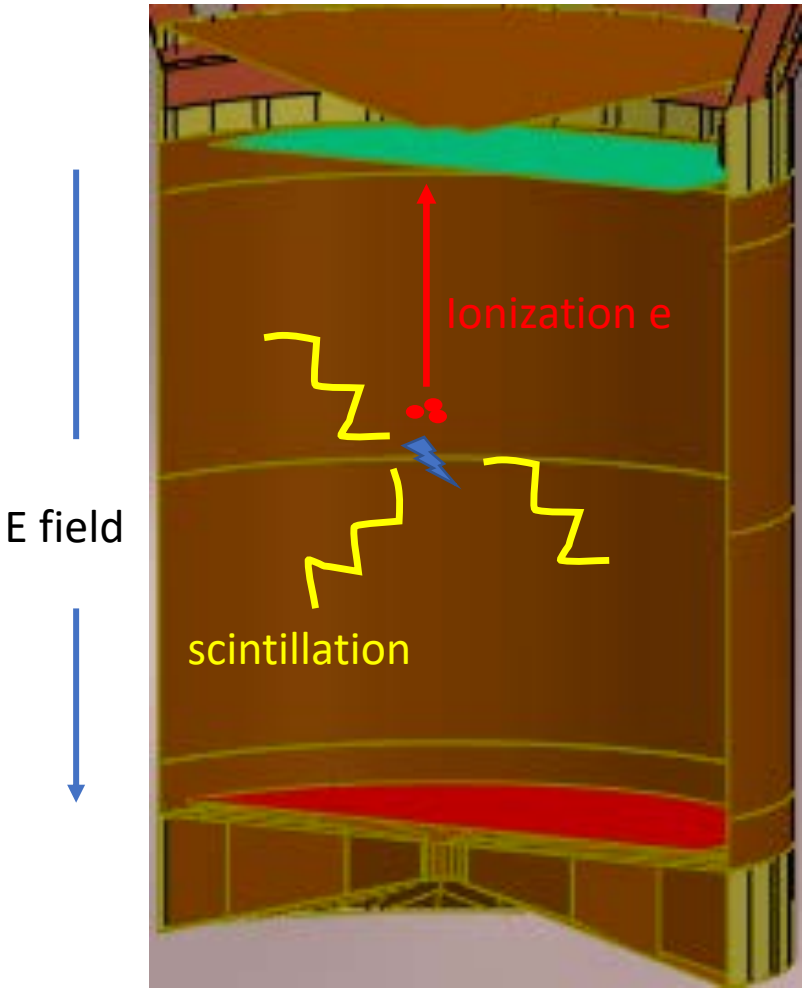

Measured diffusion coefficient versus electric field in EXO-200 and measurement from T. Doke and collaborators

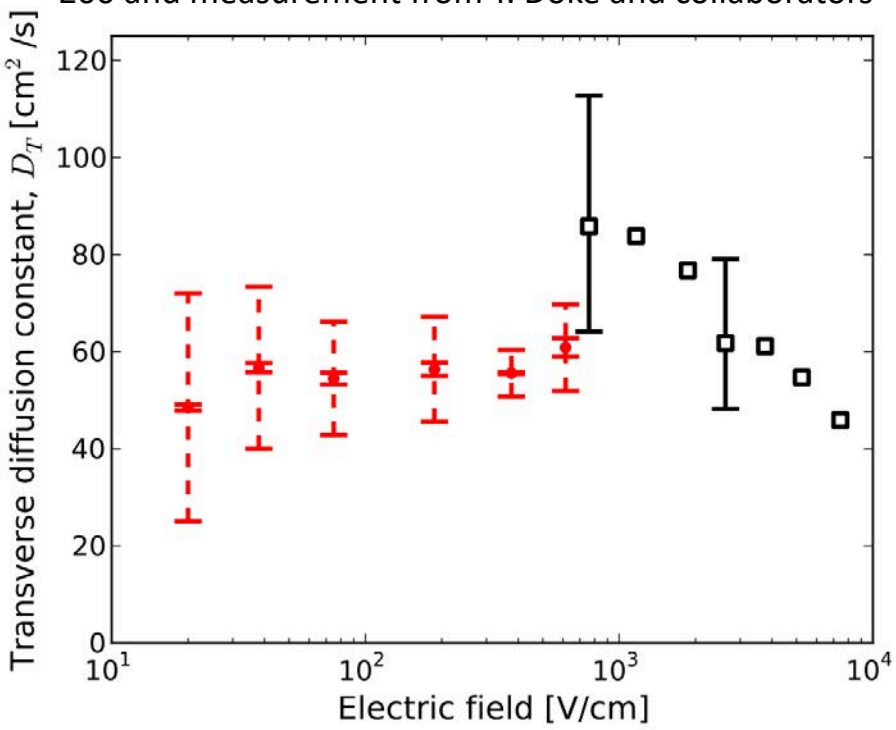

Charge signal readout in LXe TPC

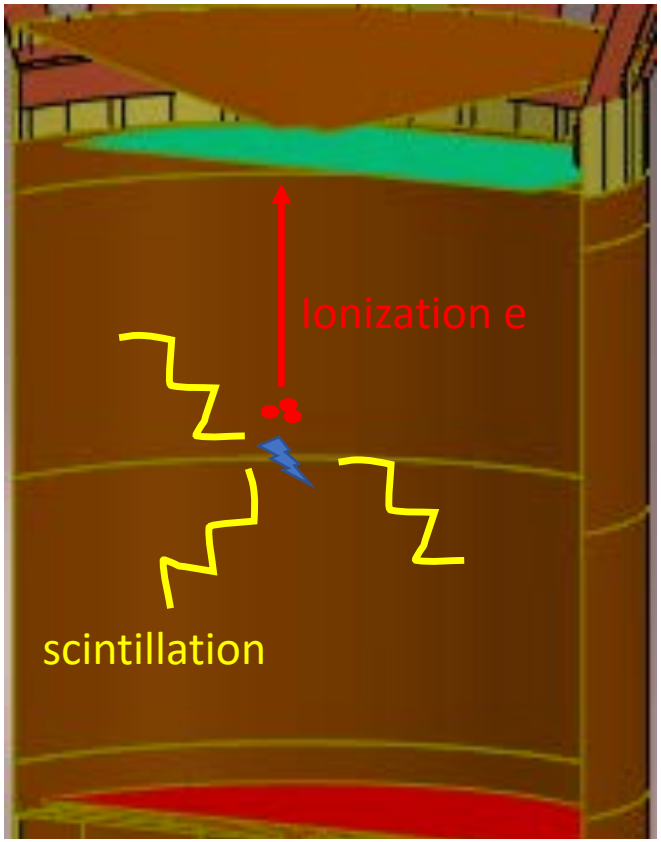

E field

Electron longitudinal diffusion coefficient versus drift field in LXe

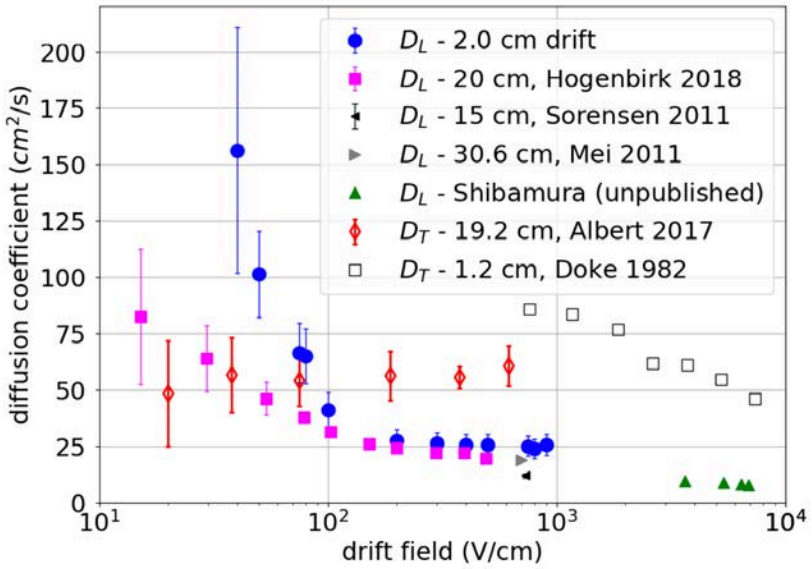

$$n(\vec{x},t) = \frac{N}{8D_T\sqrt{D_L}[\pi(t-t_0)]^{3/2}}\exp\left[\frac{-(x-x_0)^2-(y-y_0)^2}{4D_T(t-t_0)}\right]\exp\left[\frac{-([z-z_0]-v_d[t-t_0])^2}{4D_L(t-t_0)}\right]$$

Charge signal readout in LXe TPC

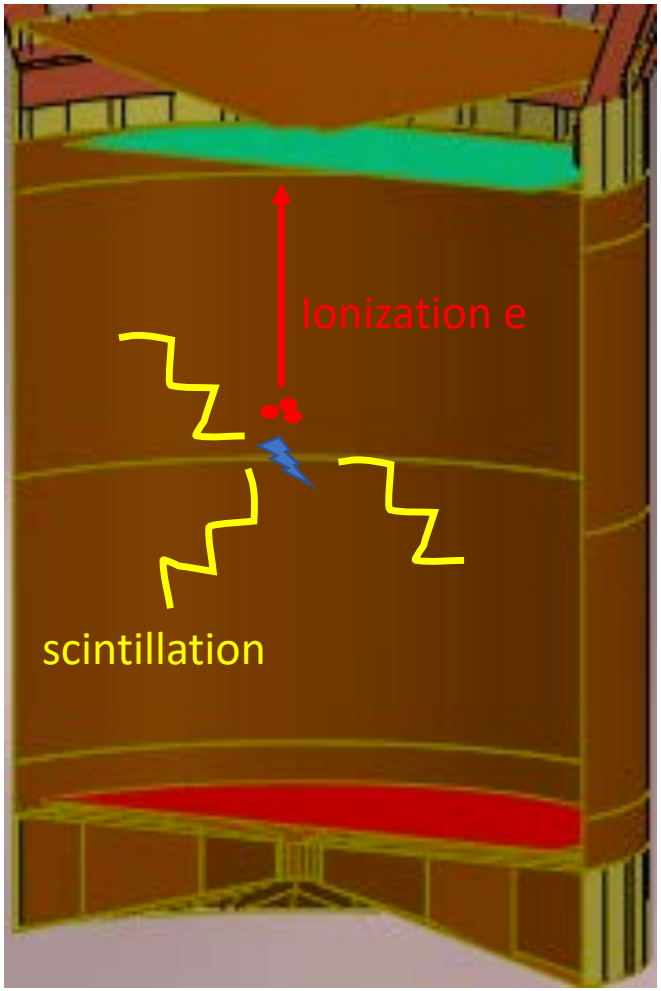

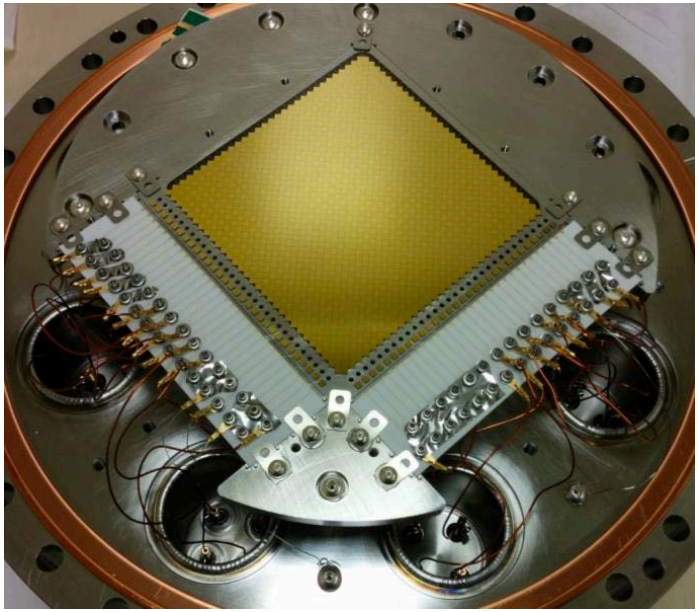

Prototype charge tile for charge readout

Ionization electrons produce induced signal on the charge tile and get collected on it at the end.

Chacterization of charge tile

- 3.3 cm of drift length, operating at up to 1kV/cm field
- Charge tile anode with 30 X strips + 30 Y strips
- PMT for light detection

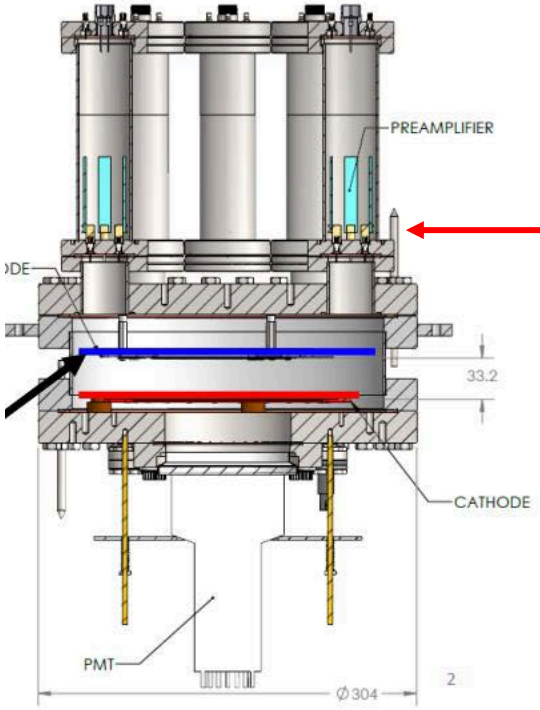

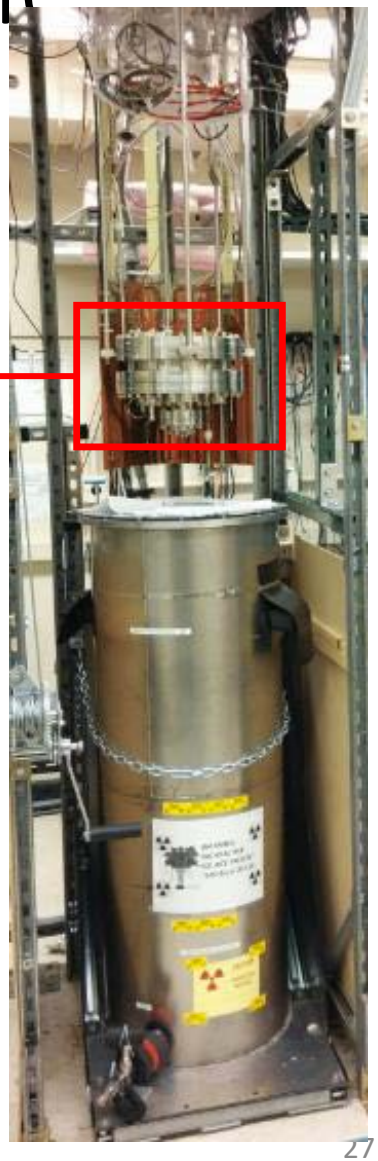

Test stand at Stanford

Characterization of charge tile

PMT (trigger)

Charge collection

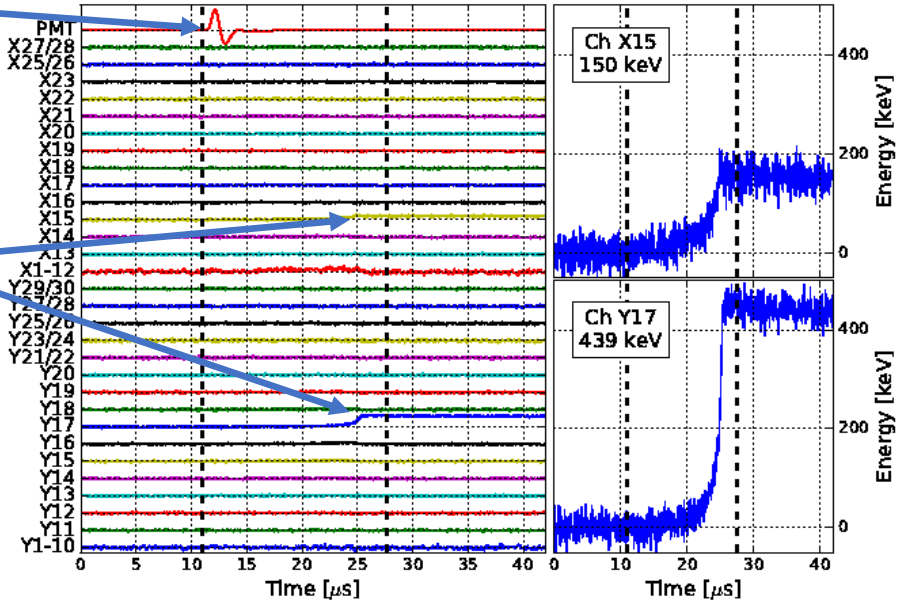

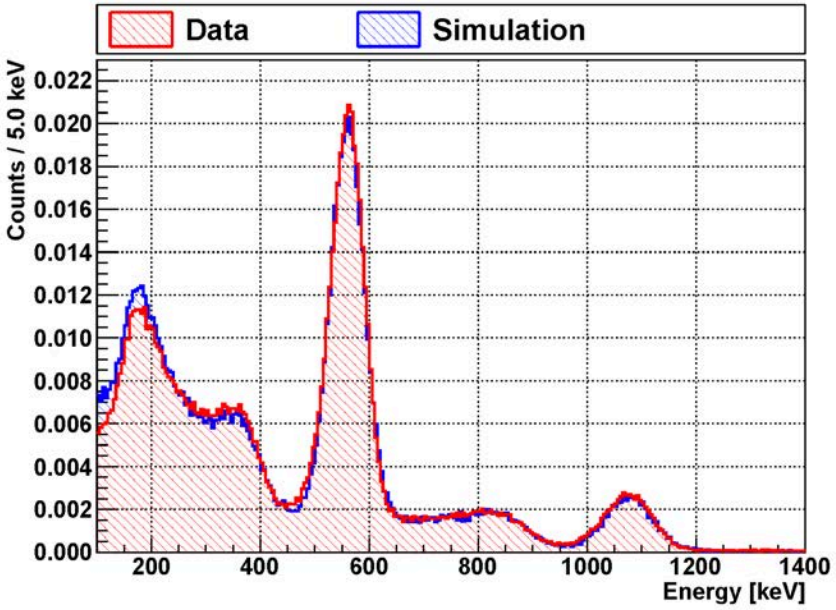

Very good agreement is achieved between the measured ionization spectrum of a ^{207}Bi source and simulations.

Simultaneous readout of charge and photon in a prototype

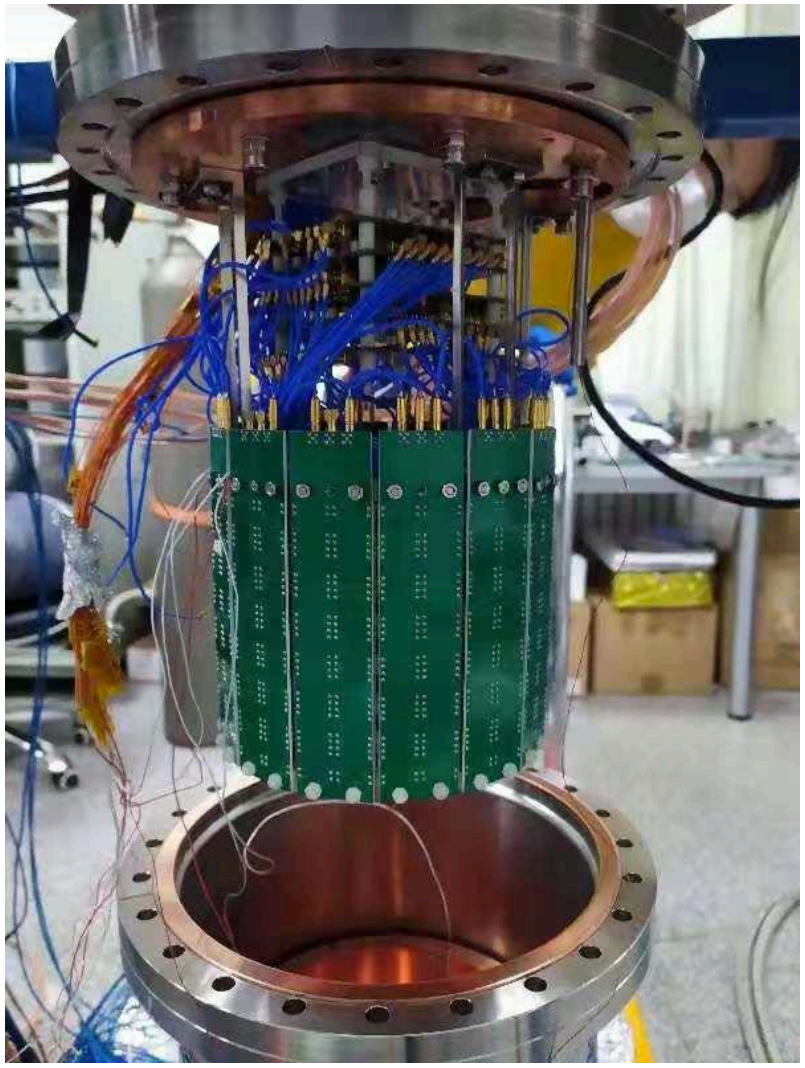

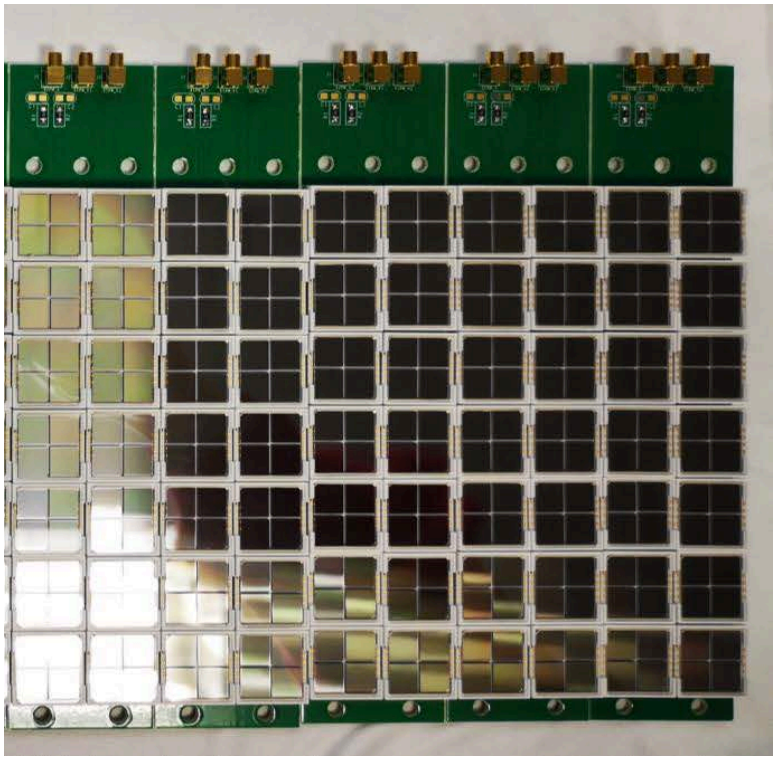

Charge tile and SiPM staves are being tested. Plan to finish assemble and take data early next year.

Simulation of charge readout in nEXO

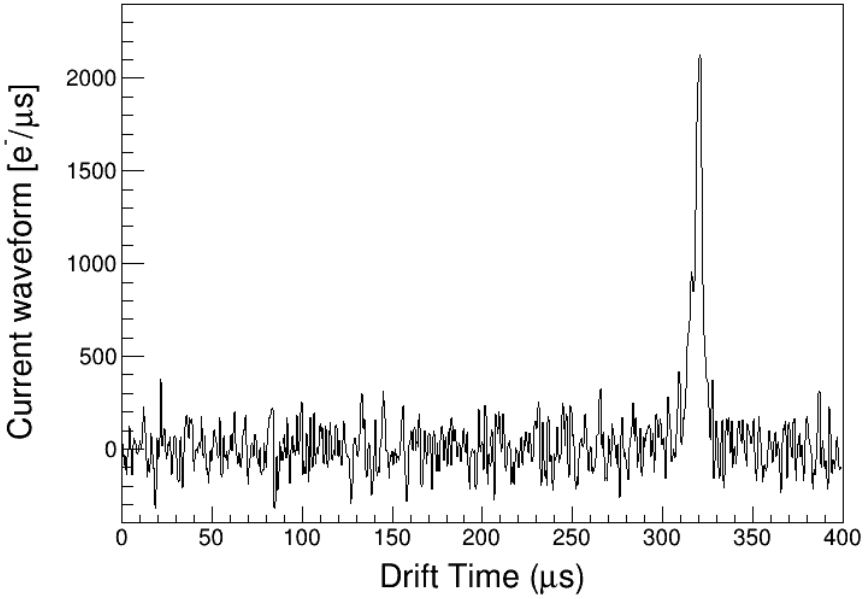

An example current waveform with 2 MHz sampling rate produced in the simulation.

- Electron drift, transverse and longitudinal diffusion are modeled in the simulation based on measurements in LXe.
- Electron lifetime is assumed to be 10 ms to model the electron attenuation.
- Each channel is added a noise that has a RMS of 200 e^-.
- A current waveform with 2 MHz sampling rate is saved for a simulated channel.

Event classification with BDT

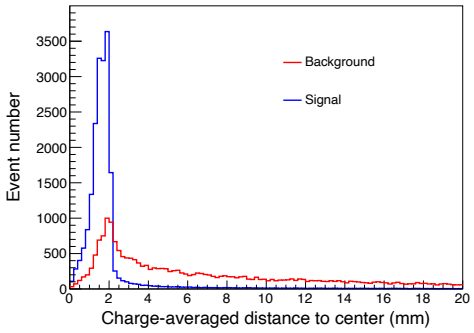

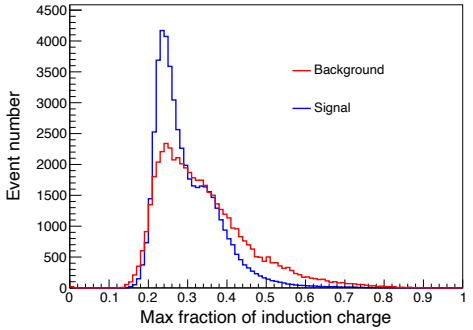

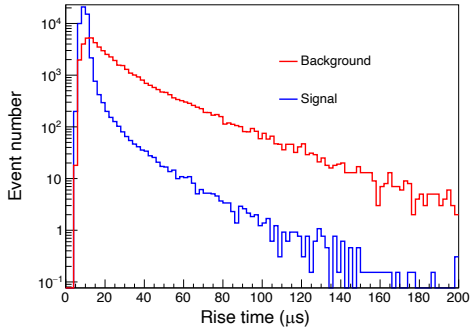

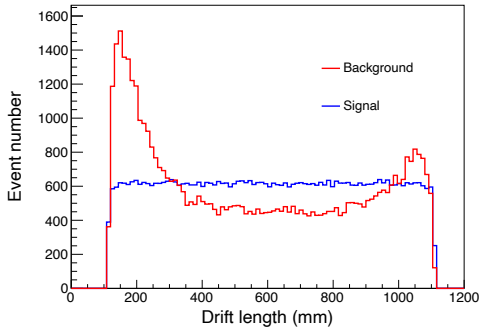

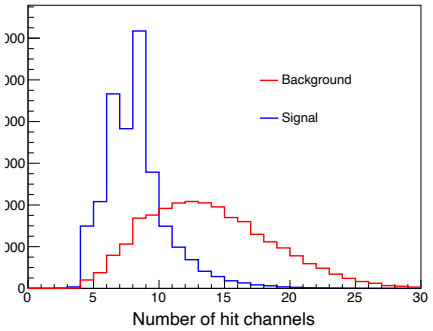

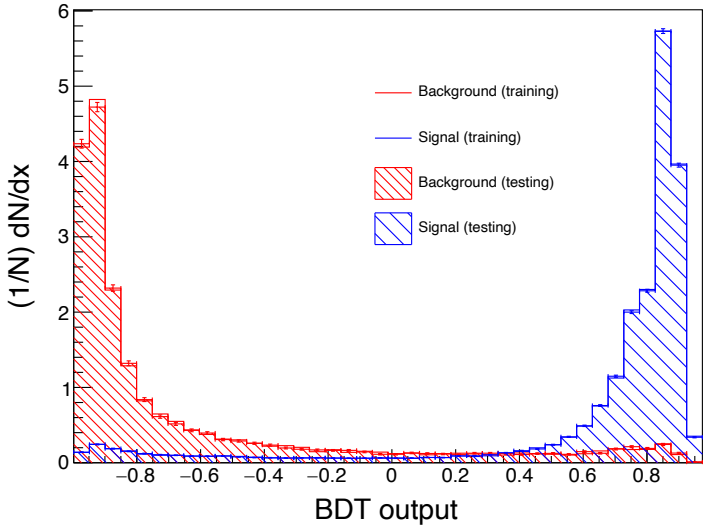

Six variables: event size in x/y, max fraction of energy on single channel, rising time, drift length, number of hit channels.

Construct a deep neural network for signal/background ID in nEXO

- Nvidia GPUs on Yale cluster are used. PyTorch 1.0 installed with conda.
- ResNet18 architecture is used.
- Simulated charge readout as input, output one score for each event between 0 (background) and 1 (signal).

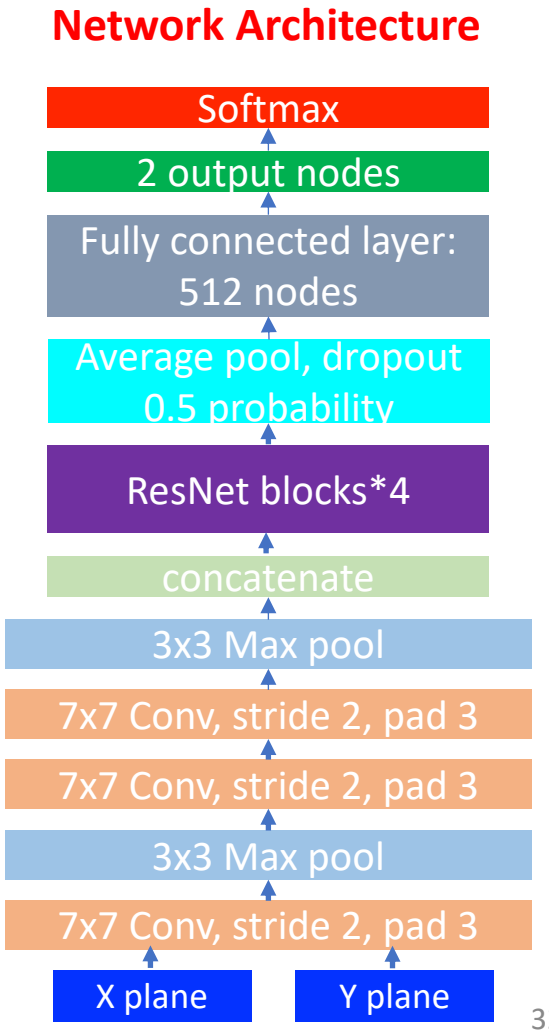

Input to neural network

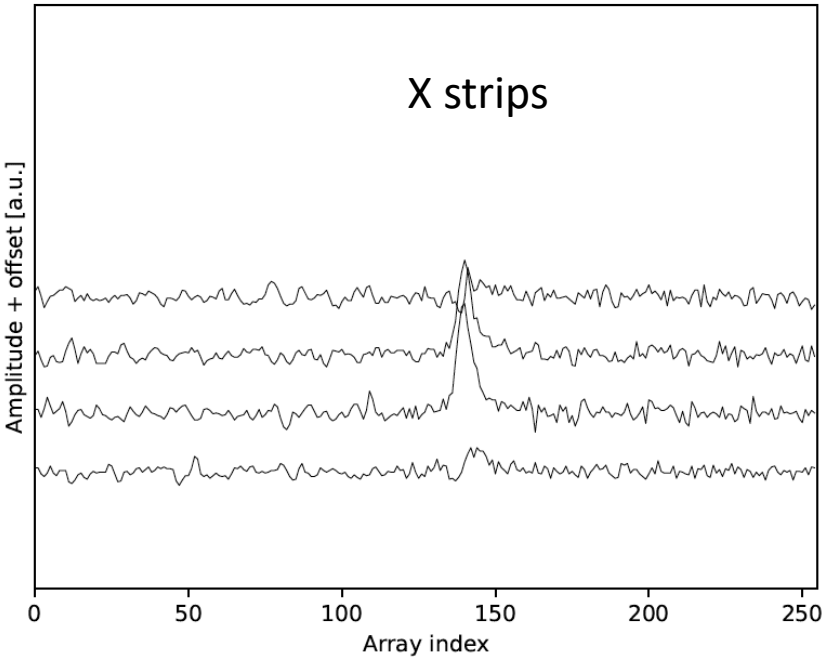

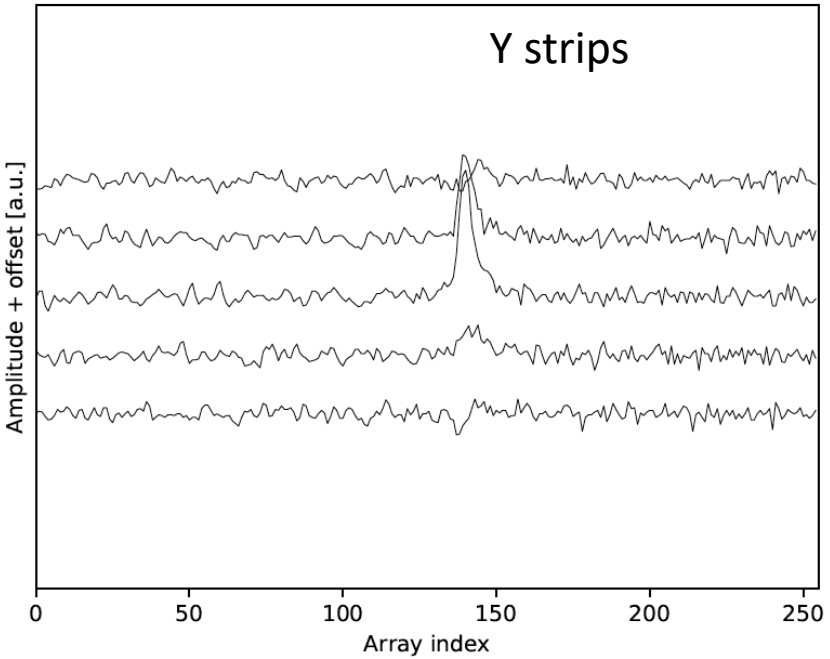

The position of X/Y strip is one index, and the time stamp of the waveform on that strip is the second index.

Signal and background events for training

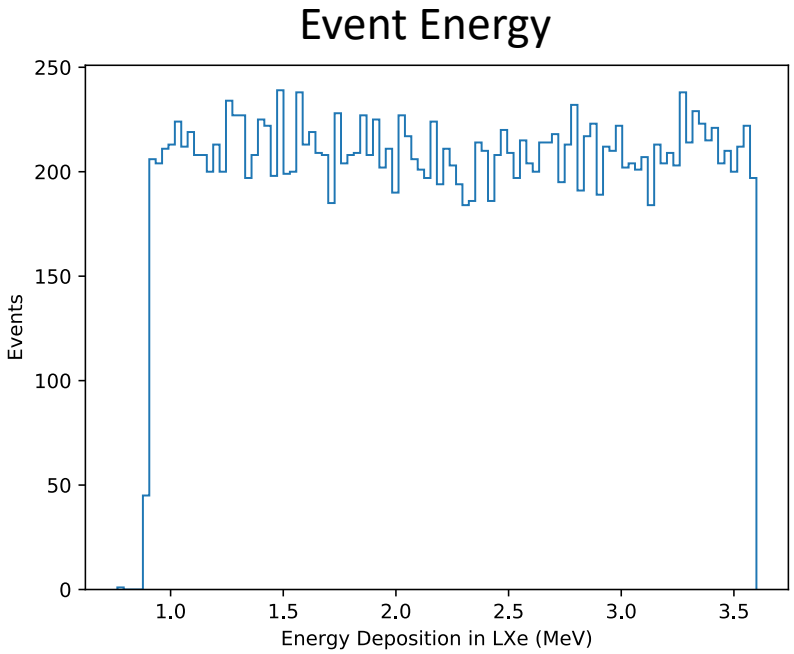

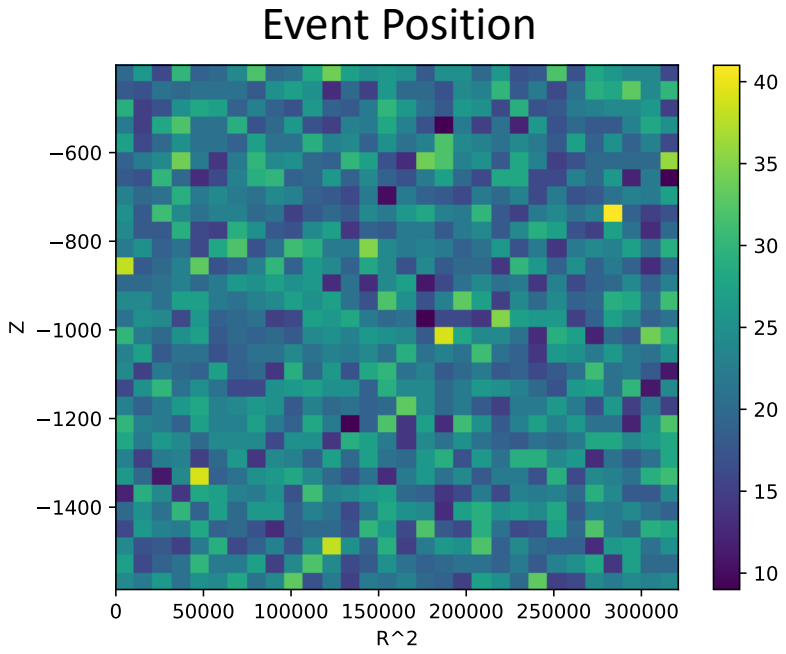

Signal and background events are generated with uniform energy and postion.

Training the network

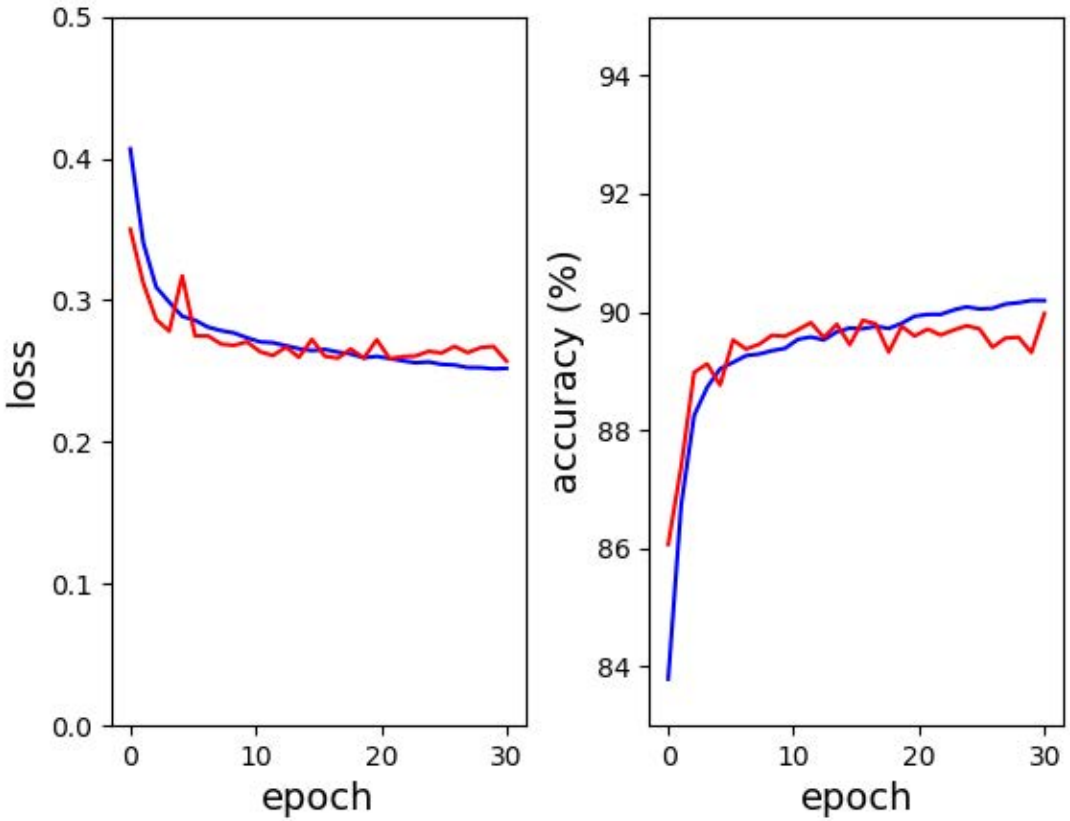

Cross entropy loss is used and accuracy is defined as ratio of correct identification.

Visualization of charge simulation events correlated to DNN score

SS-like, DNN score 0.93

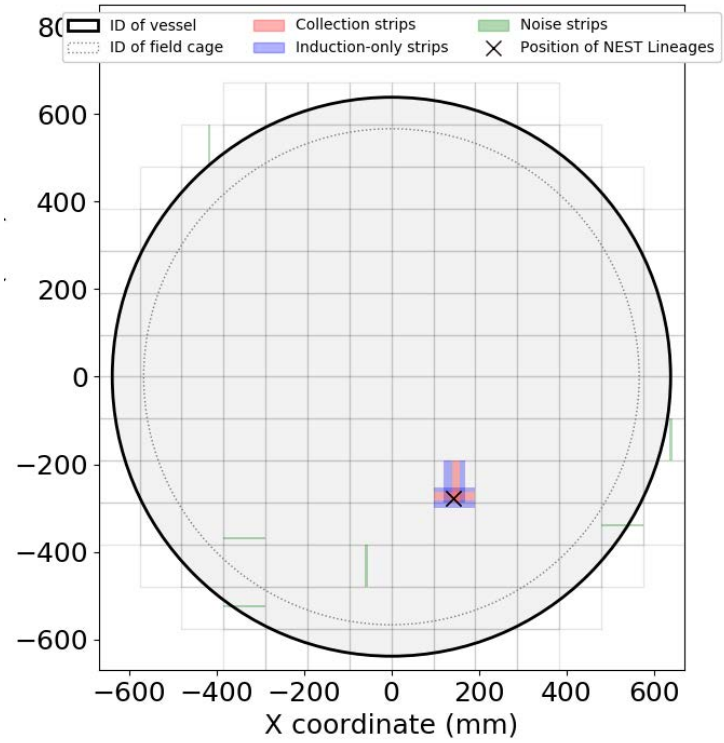

MS-like, DNN score 0.017

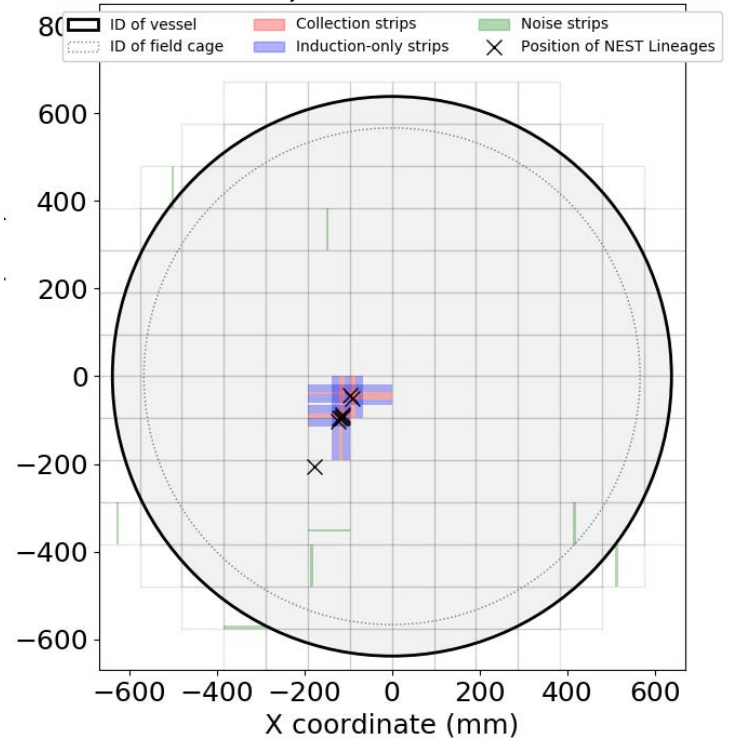

Event classification using DNN

background ← → signal

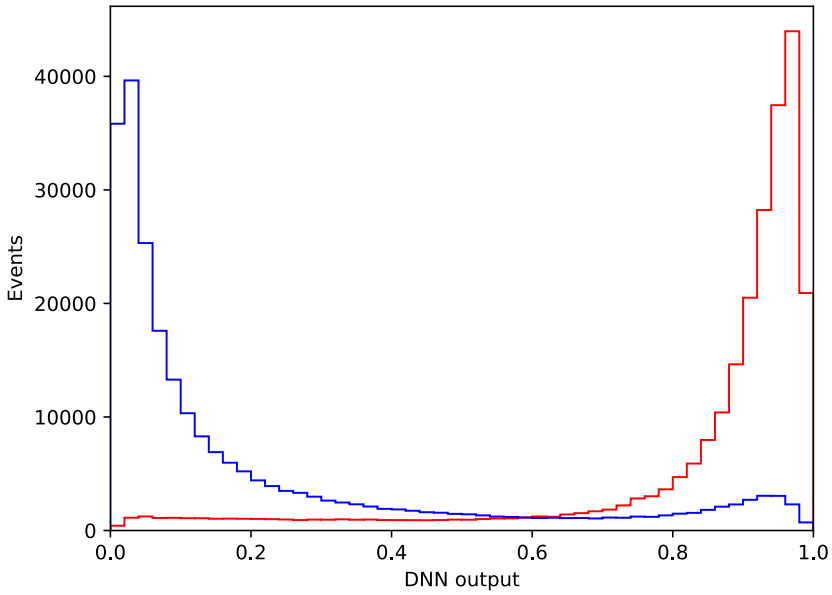

rejection efficiency
at Q value

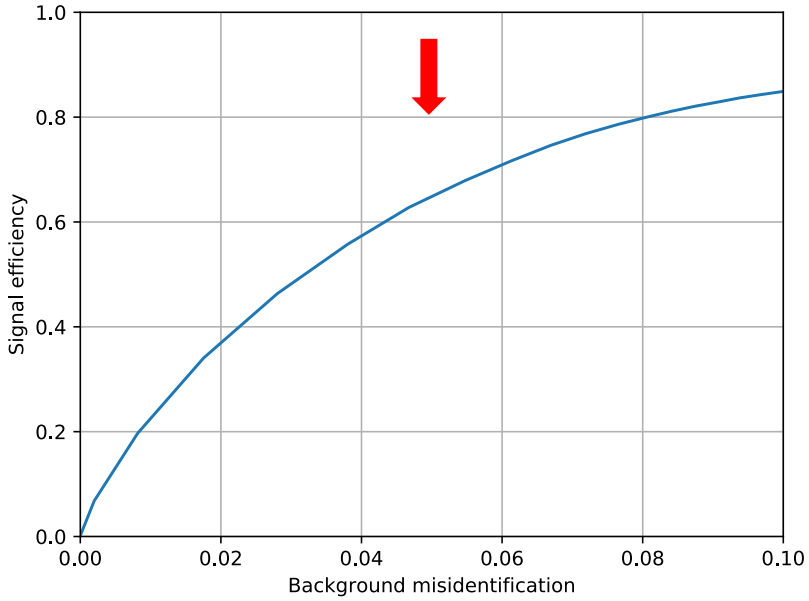

With 80% signal efficiency, the background misidentification ratio is about 8% over the energy range of 0.9-3.6 MeV.

Event classification using DNN

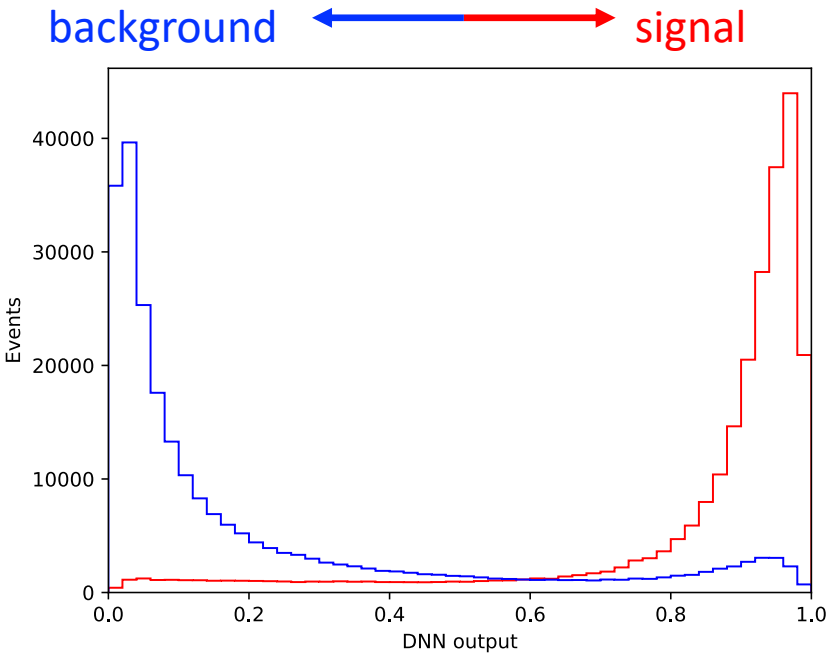

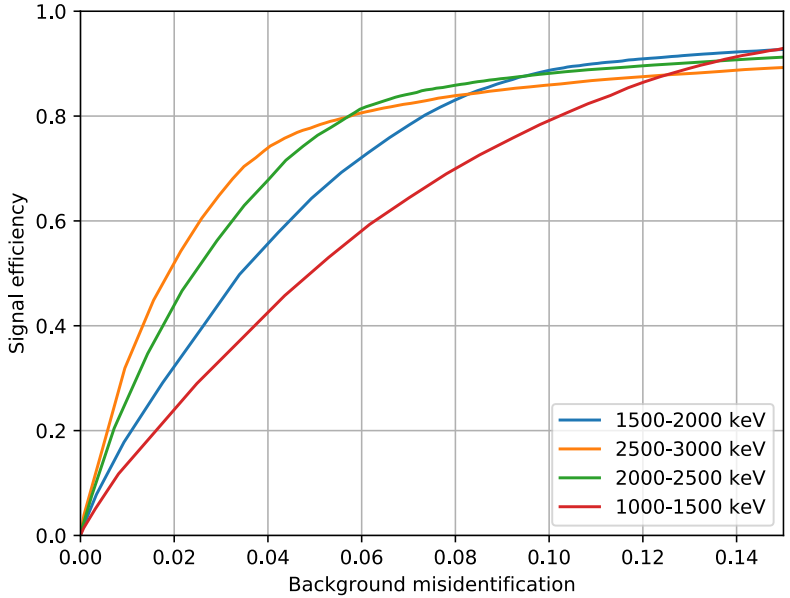

With 80% signal efficiency, the background misidentification ratio is about 5% at Q value.

Renalysis nEXO sensitivity

- We are working to reanalysis nEXO sensitivity to neutrinoless double beta decay.
- The new analysis will use the DNN event classification.

Summary

- Search for neutrinoless double beta decay is a probe to Majoron nature of neutrinos.
- EXO-200 was the first 100 kg-class experiment to run and demonstrated the power of a large and homegeneous LXe TPC.
- nEXO experiment is a tonne-scale experiment that will provide a world-leading sensitivity to neutrinoless double beta decay.

nEXO

University of Alabama, Tuscaloosa AL, USA --- M Hughes, O Nusair, I Ostrovskiy, A Piepke, AK Soma, V Veeraraghavan

University of Bern, Switzerland — J-L Vuilleumier

Brookhaven National Laboratory, Upton NY, USA — M Chiu, G Giacomini, V Radeka, E Raguzin, S Rescia, T Tsang

University of California, Irvine, Irvine CA, USA — M Moe

California Institute of Technology, Pasadena CA, USA — P Vogel

Carleton University, Ottawa ON, Canada — I Badhrees, R Gornea, C Jessiman, T Koffas, D Sinclair, B. Veenstra, J Watkins

Colorado School of Mines, Golden CO, USA --- K. Leach, C. Natzke

Colorado State University, Fort Collins CO, USA --- C Chambers, A Craycraft, D Fairbank, W Fairbank Jr, A Iverson, J Todd

Drexel University, Philadelphia PA, USA --- MJ Dolinski, P Gautam, E Hansen, YH Lin, E Smith, Y-R Yen

Duke University, Durham NC, USA — PS Barbeau, J Runge

Friedrich-Alexander-University Erlangen, Nuremberg, Germany --- G Anton, J Hoessl, T Michel, M Wagenpfeil, T Ziegler

IBS Center for Underground Physics, Daejeon, South Korea — DS Leonard

IHEP Beijing, People's Republic of China — G Cao, W Cen, Y Ding, X Jiang, P Lv, Z Ning, X Sun, T Tolba, W Wei, L Wen, W Wu, J Zhao

IME Beijing, People's Republic of China — L Cao, X Jing, Q Wang

ITEP Moscow, Russia — V Belov, A Burenkov, A Karelin, A Kobyakin, A Kuchenkov, V Stekhanov, O Zeldovich

University of Illinois, Urbana-Champaign IL, USA --- D Beck, M Coon, J Echevers, S Li, L Yang

Indiana University, Bloomington IN, USA --- JB Albert, SJ Daugherty, G Visser

Laurentian University, Sudbury ON, Canada — B Cleveland, A Der Mesrobian-Kabakian, J Farine, C Licciardi, A Robinson, U Wichoski

Lawrence Livermore National Laboratory, Livermore CA, USA --- J Brodsky, M Heffner, A House, S Sangiorgio, T. Stiegler

University of Massachusetts, Amherst MA, USA --- S Feyzbakhsh, D Kodroff, A Pocar, M Tarka

McGill University, Montreal QC, Canada --- S Al Kharusi, T Brunner, L Darroch, T McElroy, K Murray, T Totev,

University of North Carolina, Wilmington, USA — T Daniels

Oak Ridge National Laboratory, Oak Ridge TN, USA — L Fabris, RJ Newby

Pacific Northwest National Laboratory, Richland, WA, USA — I Arnquist, EW Hoppe, JL Orrell, G Ortega, C Overman, R Saldanha, R Tsang

Rensselaer Polytechnic Institute, Troy NY, USA — E Brown, K Odgers

Université de Sherbrooke, Sherbrooke QC, Canada --- F Bourque, S Charlebois , M Côté, D Danovitch, H Dautet, R Fontaine, F Nolet, S Parent, JF Pratte, T Rossignol, J Sylvestre, F Vachon

SLAC National Accelerator Laboratory, Menlo Park CA, USA --- S Delaquis, A Dragone, G Haller, LJ Kaufman, B Mong, A Odian, M Oriunno, PC Rowson, K Skarpaas

University of South Dakota, Vermillion SD, USA --- T Bhatta, A Larson, R MacLellan

Stanford University, Stanford CA, USA --- J Dalmasson, R DeVoe, G Gratta, M Jewell, S Kravitz, B.Lenardo, G Li, M Weber, S Wu

Stony Brook University, SUNY, Stony Brook NY, USA --- K Kumar, O Njoya

Technical University of Munich, Garching, Germany --- P Fierlinger

TRIUMF, Vancouver BC, Canada --- J Dilling, P Gumplinger, R Krücken, Y Lan, F Retière, V Strickland

Yale University, New Haven CT, USA — A Jamil, Z Li, D Moore, Q Xia

Backup Slides

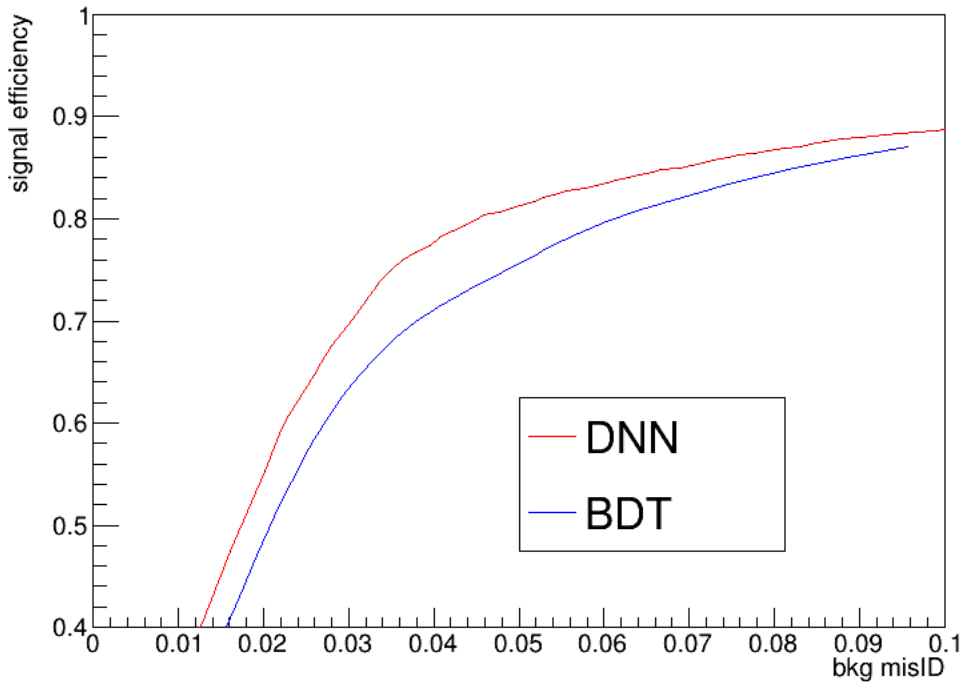

Signal and background events for training

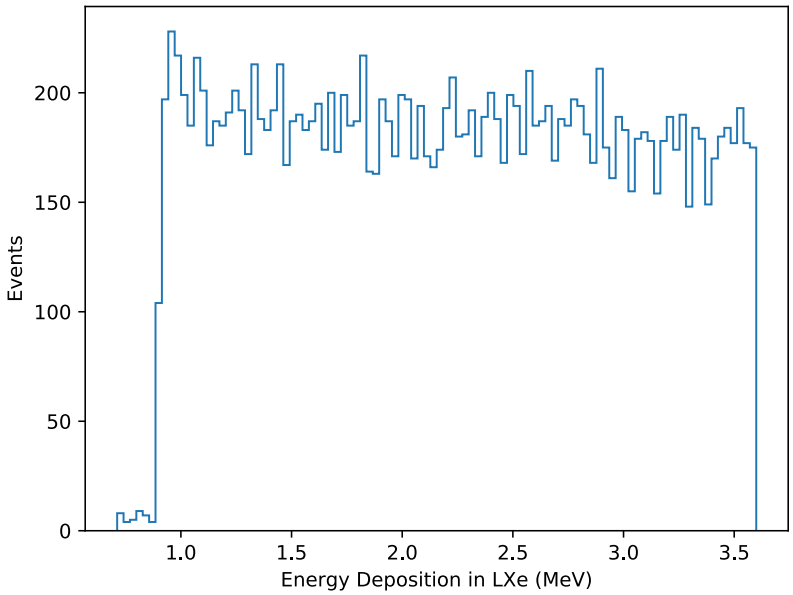

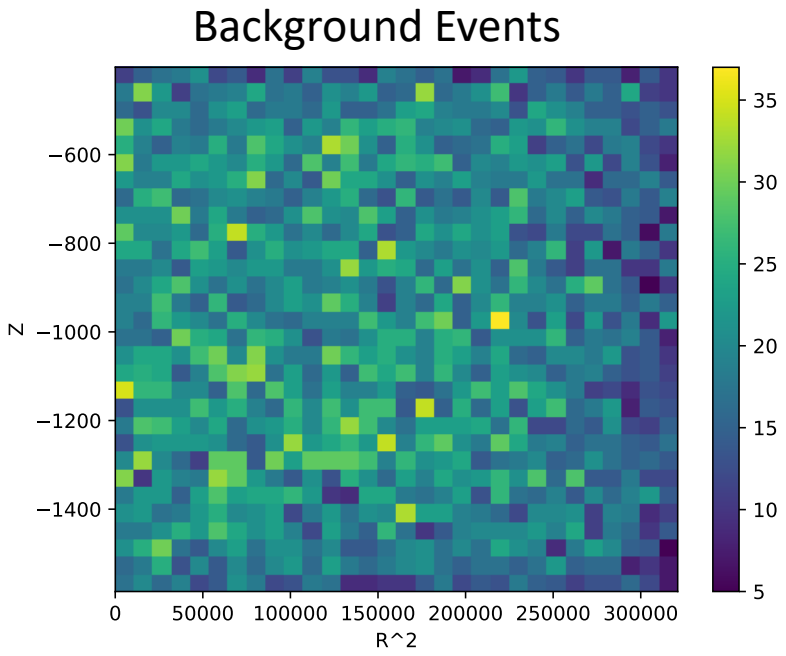

The signal and background events are uniform in the active region.

Event tagging with trained network

bb0n

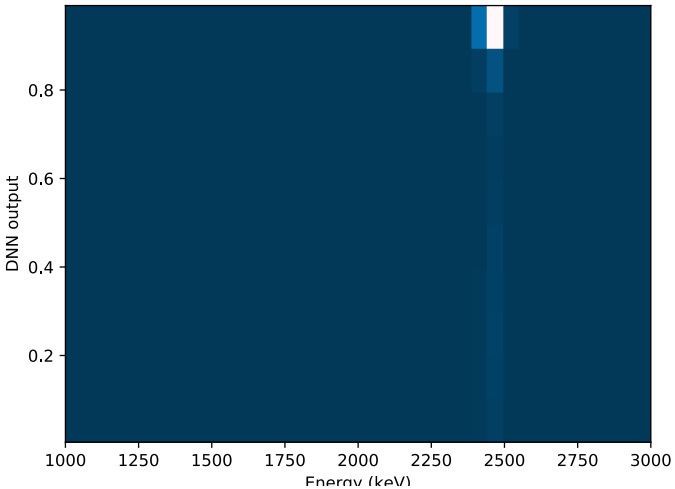

Bi214

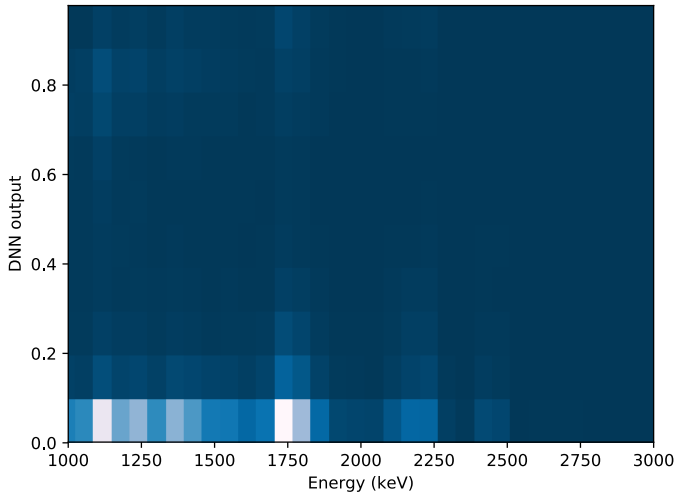

Tl208

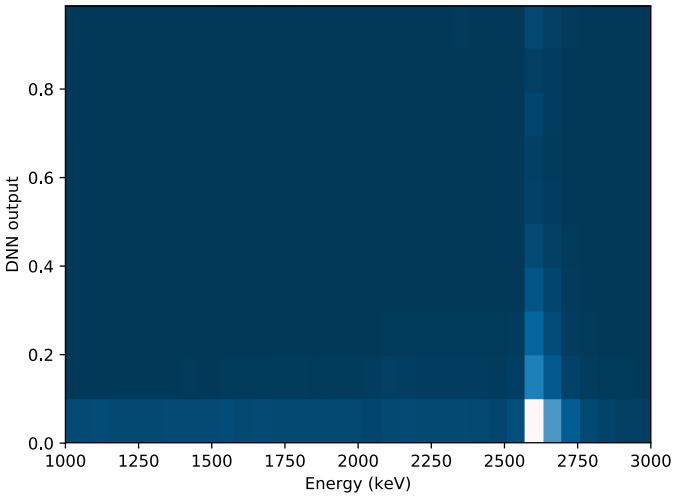

The network works properly in the energy range between 1000 keV and 300 keV.

Background rejection efficiency with DNN

bb0n vs Bi214

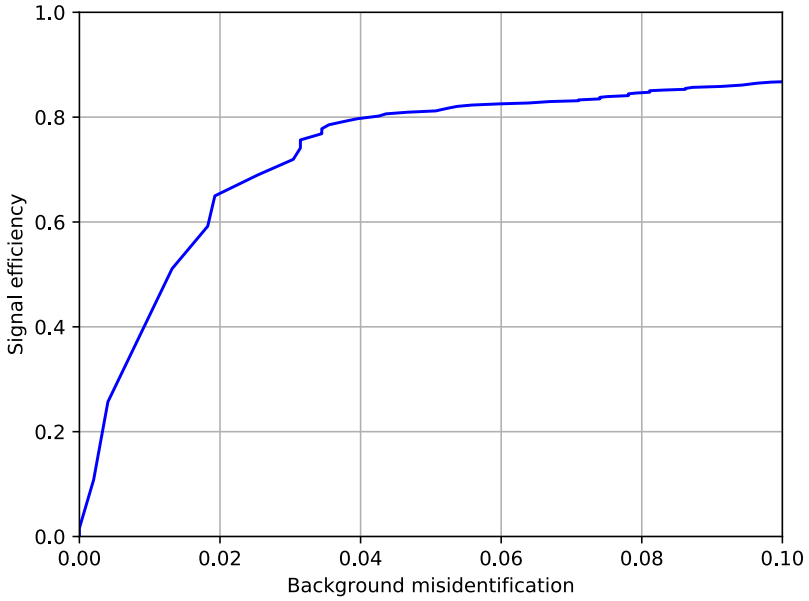

bb0n vs Tl208

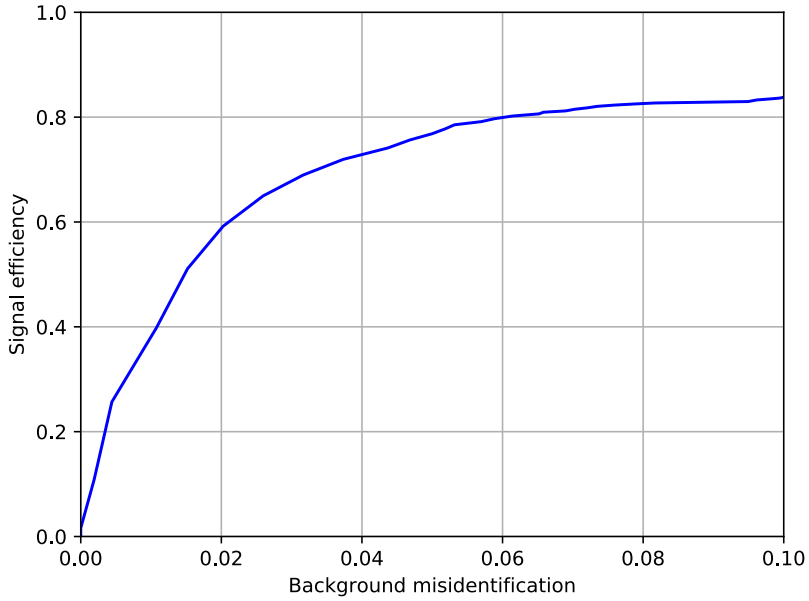

SS/MS separation for events within ROI is better for Bi214 events than Tl208 because Tl208 events within ROI are compton scatterings with escaping particles that has possibility to be single site.

With 80% signal efficiency, we can get a background misidentification ratio of 4-6%.

Dataset building/loading

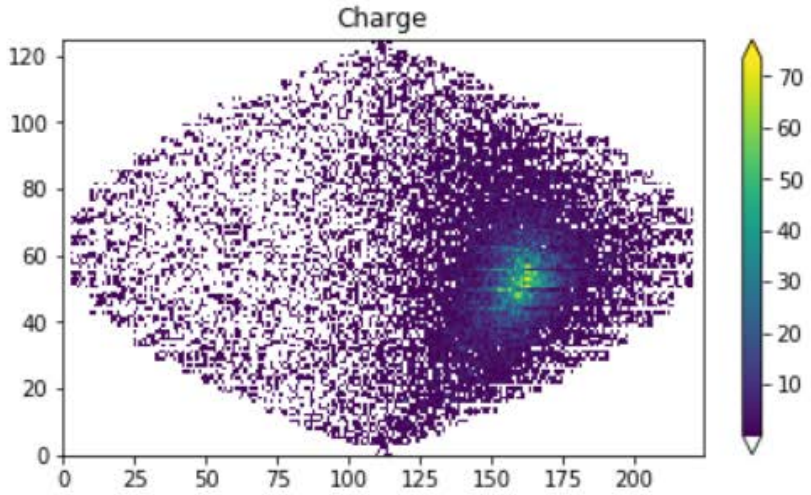

Charge in electrons

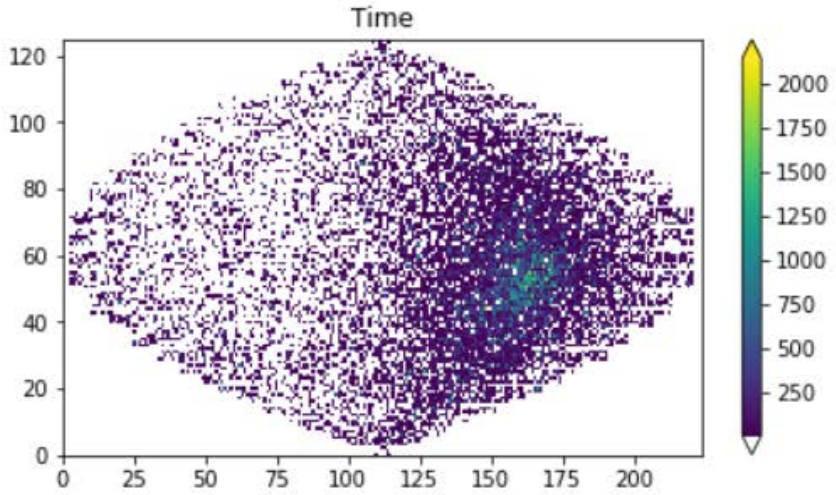

First hittime in ns

DNN-based vertex reconstruction in JUNO

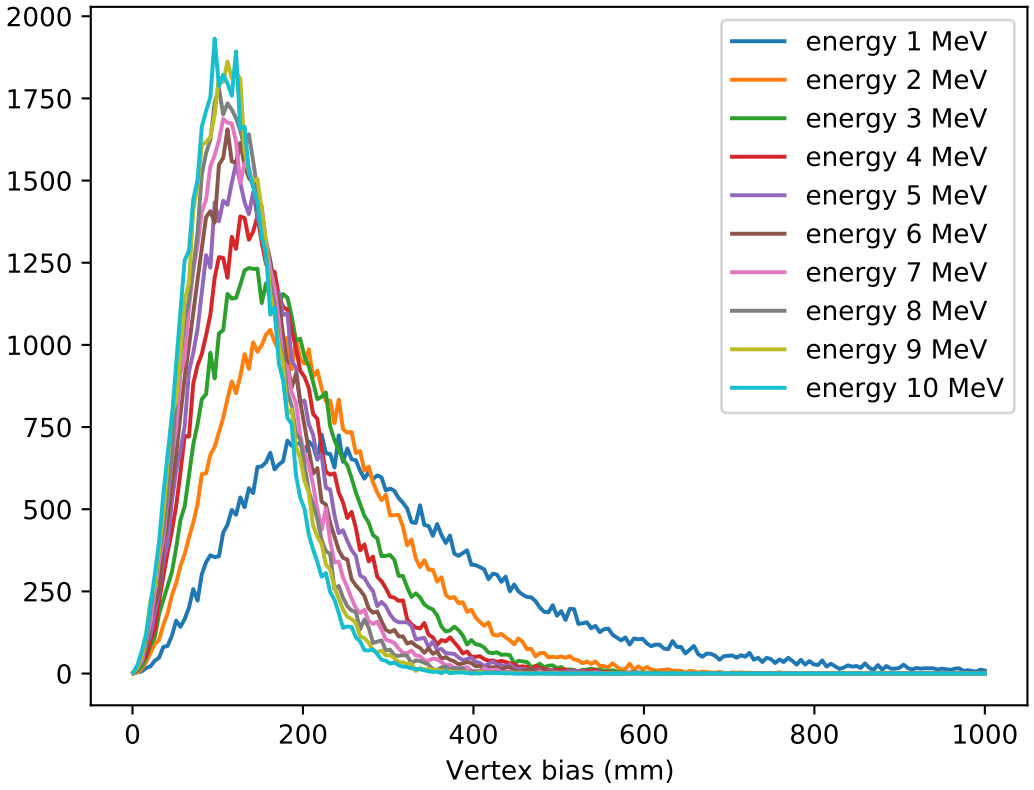

DNN event classifier for DSNB neutrino search